TECTONICS, VOL.16, NO. 2, PAGES 239-258, APRIL 1997

Growth of the South Pyrenean orogenic wedge

Andrew J. Meigs
Division of Geological and Planetary Sciences, California Institute of Technology, Pasadena

Douglas W. Burbank
Department of Earth Sciences, University of Southern California, Los Angeles

Abstract. A six-step reconstruction of the South Pyrenean foreland fold-and-thrust belt in Spain delineates the topographic slope, basal décollement angle, internal deformation, and thrust-front advance from the Early Eocene until the end of contractional deformation in the Late Oligocene. Style of thrust-front advance, dip of the basal décollement, slope of the upper surface, and internal deformation are decoupled and not simply related. Internal deformation increased, decreased, and maintained surface slope angle at different stages. From the onset to the cessation of deformation, the basal décollement angle decreased overall suggesting translation of the thrust belt onto stronger crust with time. Taper angle of the Pyrenean thrust wedge was fundamentally controlled by the flexural rigidity of the lower plate, the relative rate of creation of structural relief in the rear versus the front of the wedge, the extent of deposition of eroded material within the deforming wedge, and the taper of the pretectonic stratigraphic wedge.

Introduction

One of the most significant, and controversial, theories for fold-and-thrust belt development during the past 20 years is the critical-taper wedge model [*Chapple*, 1978; *Davis et al.*, 1983; *Stockmal*, 1983; *Davis and Engelder*, 1985; *Platt*, 1986; *Dahlen and Suppe*, 1988; *Jaumé and Lillie*, 1988; *Dahlen*, 1990; *Colletta et al.*, 1991; *Davis and Lillie*, 1994]. Mechanical properties of rocks within the thrust wedge, spatial and temporal patterns of deformation, and topographic evolution are coupled according to the model. Thrust-belt growth revolves around maintenance of a critical taper angle between the basal décollement and the surface slope. Feedback between internal deformation, which acts to build taper, and frontal accretion, tectonic thinning, and erosion, which act to decrease taper, dictates the kinematic history of a critically tapered fold-and-thrust belt. Only rarely is data from the geologic record of sufficient resolution to permit simultaneous calibration of material properties, deformational patterns, patterns of syntectonic erosion and deposition, and topography [*DeCelles and Mitra*, 1995]. As a consequence, the model is generally thought to be applicable based on qualitative compatibility between spatial and temporal patterns of thrusting in some orogens and the distribution of deformation predicted by critical-taper models [*Boyer and Geiser*, 1987; *Geiser and Boyer*, 1987; *Morley*, 1988; *Lucas*, 1989; *Boyer*, 1992; *Burbank et al.*, 1992b; *DeCelles et al.*, 1993; *DeCelles*, 1994; *DeCelles and Mitra*, 1995]. Others have argued, in contrast, that critical-taper models have limited applicability to fold-and-thrust belts because of mechanical and deformational incompatibilities between the geologic record and the model [*Woodward*, 1987; *Price*, 1988; *Meigs and Burbank*, 1993; *Bombolakis*, 1994].

This paper is a retreat to geologic data from the South Pyrenean foreland fold-and-thrust belt in Spain. A uniquely high-resolution record of deformation and topography, contained within sediments deposited during thrusting, enables detailed reconstruction of the structural and topographic development of this orogen. An increasingly popular approach is to interpret the deformational and depositional histories of thrust belts in terms of critical-taper maintenance [*DeCelles and Mitra*, 1995]. Our approach, in contrast, is to determine (1) how taper angle varies through time and (2) how that variation relates to spatial and temporal patterns of deformation, erosion, and deposition. We present a six-part sequential restoration that recovers the predeformational geometry of the thrust belt from its present, postdeformational geometry. Each sequential restoration is a time slice constrained by abundant surface and subsurface geologic data and absolute age data from syntectonic sediments. The surface slope and basal décollement varied independently and caused continuous taper-angle variation with time.

Geological Predictions of the Critical-Taper Wedge Model

In order that evolution of the Spanish Pyrenees be compared with the critical-taper wedge model, explicit definition of the model and of the geometric-kinematic predictive framework it provides is required. Six variables define the boundary conditions of the model. Two define the taper angle itself: (1) the dip of basal décollement and (2) the surface slope; three determine the critical-taper value for a specific belt: (1) the strength of material within the wedge, (2) the strength of the material within which the basal décollement is localized, and (3) the pore fluid pressure throughout the wedge; the final variable, the backstop, provides the push on and geometry of the rear of the wedge [*Chapple*, 1978; *Davis et al.*, 1983; *Stockmal*, 1983; *Davis and Engelder*, 1985; *Platt*, 1986; *Byrne and Hibbard*, 1987; *Mulugeta and Koyi*, 1987; *Dahlen and Suppe*, 1988; *Jaumé and Lillie*, 1988; *Mulugeta*, 1988; *Dahlen*, 1990; Colletta *et al.*, 1991; *Byrne et al.*, 1993; *Davis and Lillie*, 1994]. If thrust-belt development follows critical-taper wedge theory, a critical angle between the topographic slope and the basal décollement must be maintained [*Davis et al.*, 1983; *Stockmal*, 1983; *Davis and Engelder*, 1985; *Platt*, 1986; *Dahlen and Suppe*, 1988; *Jaumé and Lillie*, 1988; *Dahlen*, 1990; *Davis and Lillie*, 1994]. Patterns of

Paper number 96TC03641.
0278-7407/97/96TC-03641$12.00

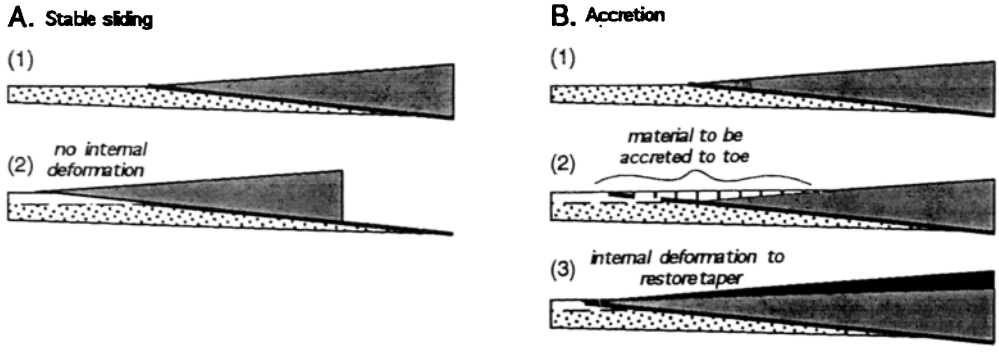

Figure 1. Schematic diagram contrasting modes of thrust-front advance. (a) A stable-sliding advance (position 2) from an initial position (position 1) occurs concurrently with aggradation of material in front of advancing wedge (open dot pattern). In the absence of erosion, accretion, or extension, the wedge maintains its taper. (b) Thrust-front advance by accretion (position 3) occurs after aggradation of material in front (open dot pattern) and on top (vertical line pattern) of wedge (position 2). Addition of material to front of wedge decreases taper angle.

internal deformation are modulated by changes in the surface slope and in material properties within and at the base of the wedge. Stress transmission to and accretion of material at the toe occurs only when the wedge is critically tapered.

Subcritical, critical, and supercritical are the possible wedge-taper states given by the model [*Davis et al.*, 1983]. A subcritically tapered wedge has a taper angle below that required for slip transmission on the base whereas a supercritically tapered wedge's taper angle is greater than the critical value [*Davis et al.*, 1983; *Woodward*, 1987; *Dahlen*, 1990; *Dahlen and Suppe*, 1988; *DeCelles and Mitra*, 1995]. Once a wedge has attained critical taper, two contrasting modes of thrust-front advance, that is, repositioning of the deformation front toward the foreland, are implied by the model [*Davis et al.*, 1983] (Figure 1). Translation of a critically tapered wedge along its base without addition or removal of material to either its toe or base requires no internal deformation because the taper angle is maintained (herein referred to as stable sliding; Figure 1a). Alternatively, a critically tapered wedge whose thrust-front advances by the accretion of material to its toe must experience concurrent internal deformation in order to maintain the critical taper angle (herein referred to as accretion, Figure 1b).

If periods of thrust-front advance by accretion can be differentiated from periods of stable sliding, a contemporaneous and appropriate internal deformational response is expected within the wedge. During the course of a hypothetical orogeny, the coupling between thrust front advance, internal deformation, and taper angle are illustrated in Figure 2. At time t_0 the thrust front relocates toward the foreland at the base of a tapered, stratigraphic wedge. Such an accretion event is comparable to that of initiation of the Salt Range thrust 100 km toward the foreland of the previous thrust front in the Pakistan Himalaya [*Davis and Engelder*, 1985; *Burbank and Beck*, 1989; *Davis and Lillie*, 1994]. Between t_0 and t_1, the thrust front remains fixed, internal deformation accumulates, and the taper angle builds to a critical angle (Figure 2). The history of the wedge after t_1 depends on whether the next thrust-front advance occurs by accretion or stable sliding. If the advance at t_1 is by accretion (Figure 2a), the wedge lengthens and the taper angle decreases. Like the t_0-t_1 period, the thrust front subsequently remains fixed during the t_1-t_2 interval and internal deformation rebuilds taper to the critical angle. Alternatively, if the thrust front advances by stable sliding between t_1 and t_2 (Figure 2b), the wedge remains at critical taper, internal deformation ceases, and the thrust front advances gradually toward the foreland. Although these end-members imply a simple relationship between internal deformation and thrust-front advance, they do not account for processes such as erosion, isostatic depression from loading, or tectonic thinning of the hinterland that also impact taper with time [*Davis et al.*, 1983; *Platt*, 1986; *Woodward*, 1987; *DeCelles and Mitra*, 1995].

A particular set of geologic observations are required, based on this framework, to compare a foreland fold-and-thrust belt with the critical-taper wedge model. Explicitly, the necessary geologic data that must be determined simultaneously throughout an orogeny are (1) the dip of basal décollement; (2) the dip of the topographic surface; (3) the spatial and temporal distribution of deformation; (4) the contrasting strength of materials within and at the base of the wedge (including down dip changes in the strength of the basal décollement); and (5) the pore fluid pressure. Whereas the first three variables can be constrained with confidence in the Pyrenees and the comparative strengths of rocks within the wedge and at its base can be qualitatively assessed, the pore fluid conditions can not be estimated. Below we document the changes (or lack thereof) in these variables between six well-constrained temporal and geometrical reconstructions of the Spanish Pyrenean foreland fold-and-thrust belt.

General Characteristics of the Pyrenean Wedge

Collision of the Iberian plate with European plate created a compact, two-sided orogen (Figure 3a) [*Muñoz*, 1992]. Paired foreland fold-and-thrust belts and foreland basins were formed to the north and south of the axial zone, an imbricate stack of crystalline thrust sheets. This study focused on the thrust sheets of the central segment of the Spanish Pyrenean foreland thrust belt, the South-Central Unit [*Choukroune and Seguret*, 1973; *Williams and Fischer*, 1984; *Williams*, 1985; *Muñoz*, 1992]. The South-Central Unit consists of two thrust sheets on the west (the Montsec and Sierras Marginales) and three thrust sheets on the east (the Bóixols, Montsec, and Sierras Marginales) (Figure 3b). Our analysis of a corridor parallel to the Ribagorzana River on

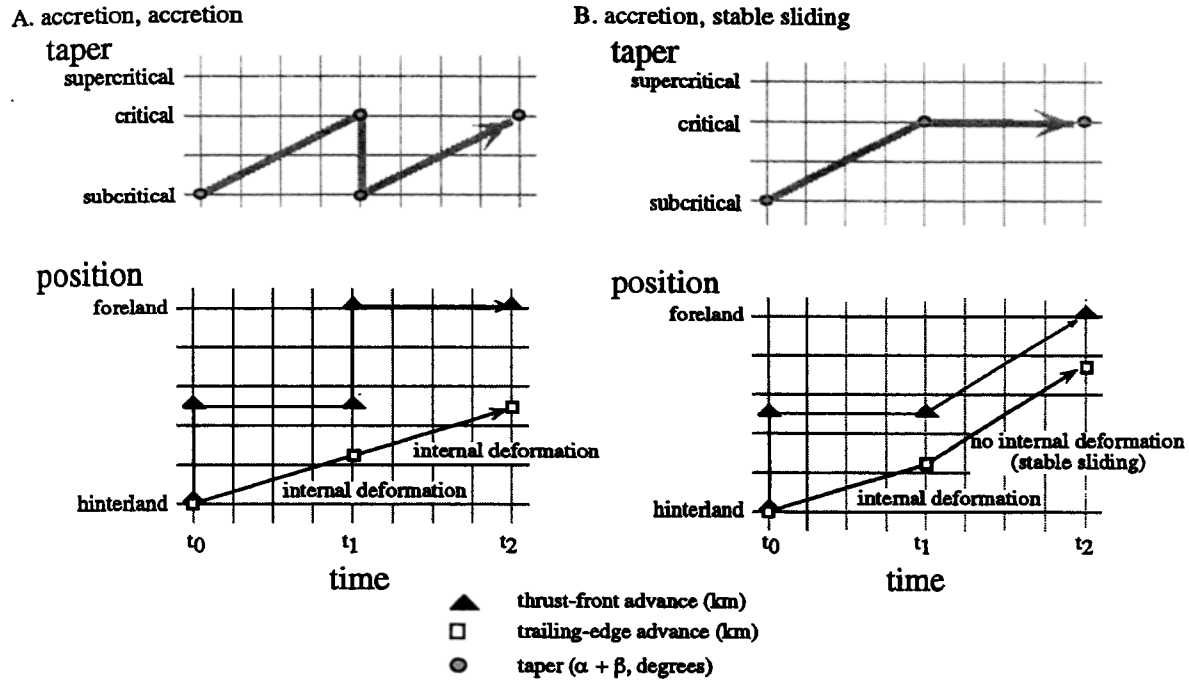

Figure 2. Plot of wedge taper and position of thrust front and trailing edge of thrust belt for accretion followed by (a) accretion and accretion followed by (b) stable sliding kinematic paths. In both cases t_0 depicts the case of instantaneous accretion such as that which occurs when the basal detachment suddenly propagates into the foreland in a stepwise fashion. Between t_0 and t_1, internal deformation builds taper to a critical angle. Note that in the case of accretion followed by accretion, the total advance of the trailing edge of the thrust belt is due to internal deformation (Figure 2a). The trailing-edge-thrust-front distance increases, decreases, increases, and decreases with time in this scenario (compare the thrust-front and trailing-edge advance curves, Figure 2a). In contrast, the trailing edge advances because of internal deformation and stable sliding in the case of accretion followed by stable sliding, respectively (Figure 2b). At t_1, the thrust-front-trailing-edge distance remains fixed (compare the thrust-front and trailing-edge advance curves, Figure 2b). Taper is the sum of ß the dip of basal décollement and a, the dip of the topographic slope.

the western side of the South-Central Unit provides an excellent area to study the evolution of an entire foreland thrust-belt system for several reasons (Figure 4). Major structures are exceptionally well exposed from the foreland across strike to the axial zone and locally have vertical exposure up to 1 km, age relationships between major and minor structures are clear [*Meigs*, 1997], and the stratigraphic framework is well established (Figure 5) [*Pocoví*, 1978a, b; *Simó and Puigdefàbregas*, 1985; *Williams*, 1985; *Senz and Zamorano*, 1992; *Meigs*, 1997]. In addition, the neighboring Etude Continentale et Oceanique par Reflexion et Refraction Sismique (ECORS) line, a deep seismic profile (Figure 3), other structural analyses in the region, and a dense array of subsurface information from well and seismic data provide tight constraints on the dip of the basal décollement, the subsurface locations of important cutoffs, and ages of units below the basal décollement [*Misch*, 1934; *Pocoví*, 1978a; *Williams and Fischer*, 1984; *Williams*, 1985; *Martínez Peña and Pocoví*, 1988; *Choukroune and ECORS Team*, 1989; *Losantos et al.*, 1989; *Roure et al.*, 1989; *Sáez et al.*, 1991; *Muñoz*, 1992; *Vergés et al.*, 1992, 1996; *Vergés*, 1993; *Senz and Zamorano*, 1992; *Meigs et al.*, 1996; *Meigs*, 1997]

A Geologic Cross Section of the Pyrenean Foreland Fold-and-Thrust Belt

A present-day cross-section of the foreland fold-and-thrust belt extends from the undeformed foreland on the south to the axial zone on the north (Figures 3, 4, and 6). Several general observations are obvious on initial inspection of the section. The Barbastro anticline is the southernmost surface expression of deformation and is related to folding at the southern tip of the basal décollement [*Martínez Peña and Pocoví*, 1988; *Losantos et al.*, 1989]. Two structural domains characterize the hanging wall structures of the Sierras Marginales thrust sheet [*Meigs*, 1997]. On the south, a dense array of imbricate thrusts substantially modified the leading edge of the sheet (Figures 4 and 6). In contrast, broad, open folds characterize structures in the hanging wall to the north of the Montargull thrust. No internal deformation is seen within the Montsec thrust sheet except on its southern edge where a disrupted anticline is preserved [*Misch*, 1934; *Williams*, 1985]. A wedge of undifferentiated sedimentary and metamorphic rocks of the axial zone mark the northern edge of the section. This axial zone wedge is seen along the strike length of the Pyrenees and is interpreted to represent the structurally highest horse in the antiformal stack duplex [*Williams and Fischer*, 1984; *Williams*, 1985; *Martínez et al.*, 1988; *Muñoz*, 1992; *Vergés*, 1993; *Vergés et al.*, 1996]. In this sense, the axial zone acted as the backstop [*Davis et al.*, 1983; *Byrne and Hibbard*, 1987; *Davis and Lillie*, 1994] in the emplacement of the foreland fold-and-thrust belt. Included in this undifferentiated backstop is the Nougats zone, a second, smaller duplex formed in Triassic and basement rocks above the uppermost horse in the axial zone duplex [*Williams*, 1985; *Muñoz*, 1992]. Two

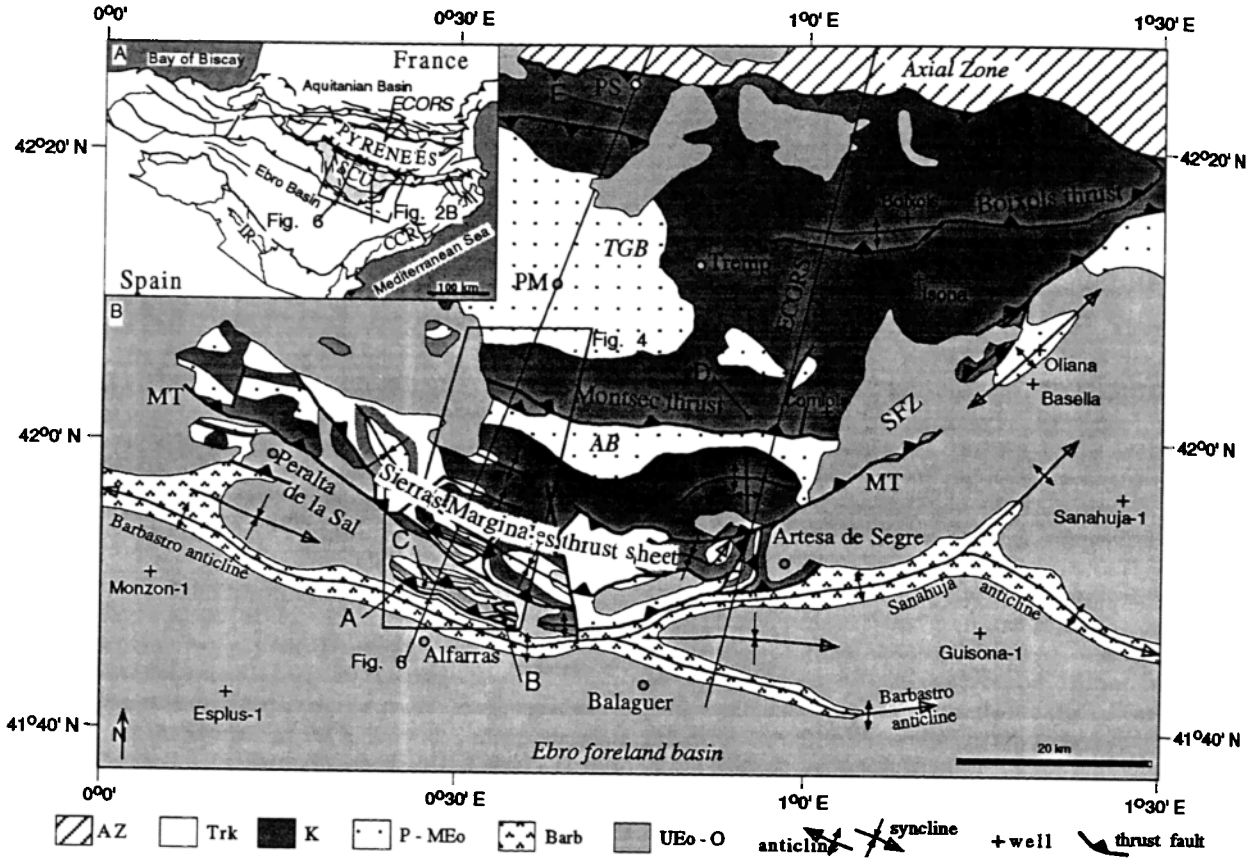

Figure 3. Location geologic maps of the Pyrenees and study area. (a) Regional tectonic map showing the major geologic features of the Pyrenean orogen. SCU identifies the south central sector of the Spanish Pyrenees (modified from *Vergés* [1993]). Note the position of the Ribagorzana cross section (Figure 6) with respect to the Etude Continentale et Oceanique par Reflexion et Refraction Sismique (ECORS) deep crustal seismic profile. The axial zone is indicated by the cross hatch pattern beneath the word Pyrenees. (b) Geologic map of the South-Central Unit of the Spanish Pyrenees. The Bóixols thrust, which has considerable displacement to the east, loses displacement to the west and is not present; only the Montsec and Sierras Marginales thrust sheets are seen (base after *Teixell* [1992]). Note that the frontal portion of the Sierras Marginales thrust sheet is partially obscured by Oligocene syntectonic strata. Key features to note are the Barbastro anticline in the foreland, interpreted to represent the leading edge of Pyrenean deformation, and the Montargull thrust (MT) within the Sierras Marginales thrust sheet. Stratigraphic sections used to construct the stratigraphic panel of figure 5 are indicated (sections A-E). SFZ denotes the mostly buried Segre Fault Zone; abbreviations are as follows: AB, Ager basin; TGB, Tremp-Graus basin; Az, undifferentiated rocks of the axial zone; Trk, Triassic evaporites; UK, Upper Cretaceous; P-MEo, Paleocene to Middle Eocene; B, Barbastro evaporites (base of the Ebro foreland basin sequence); and UEo-Oligocene, Upper Eocene to Oligocene syntectonic strata. Pretectonic rocks are the Triassic through Paleocene. The locations of Figures 4 and 6 are shown.

extensively studied Early to Middle Eocene piggyback basins, the Ager and Tremp-Graus basins, sit above the northern Sierras Marginales and Montsec thrust sheets, respectively (Figures 3, 4, and 6) [*Mutti et al.*, 1985, 1988; *Losantos et al.*, 1989; *Muñoz*, 1992].

Structural Data

Surficial structural data for the section came from two sources. Detailed mapping from foreland to the southern margin of the Tremp-Graus basin was conducted to delineate the geometries of major structures and to determine the structural and stratigraphic relationships between structure and synorogenic sediments (Figures 3 and 4). Extensive mapping in the southern portion of the study area revealed a number of key observations that define the structural sequence [*Meigs*, 1997]. This mapping was supplemented by previous structural analyses on the Sierras Marginales thrust sheet and detailed studies of the leading edge of the Montsec thrust sheet [*Misch*, 1934; *Pocovi*, 1978a; *Mutti et al.*, 1985, 1988; *Losantos et al.*, 1989]. Data for the section from the Tremp-Graus basin to the north was derived from the geologic map Catalunya [*Losantos et al.*, 1989], a previously published crustal section [*Williams*, 1985], and a detailed regional study of the crustal structure of the eastern part of the South-Central Unit [*Vergés*, 1993]. The northern part of the section greatly simplifies structure north of the trailing edge of the Montsec thrust sheet (Figure 6).

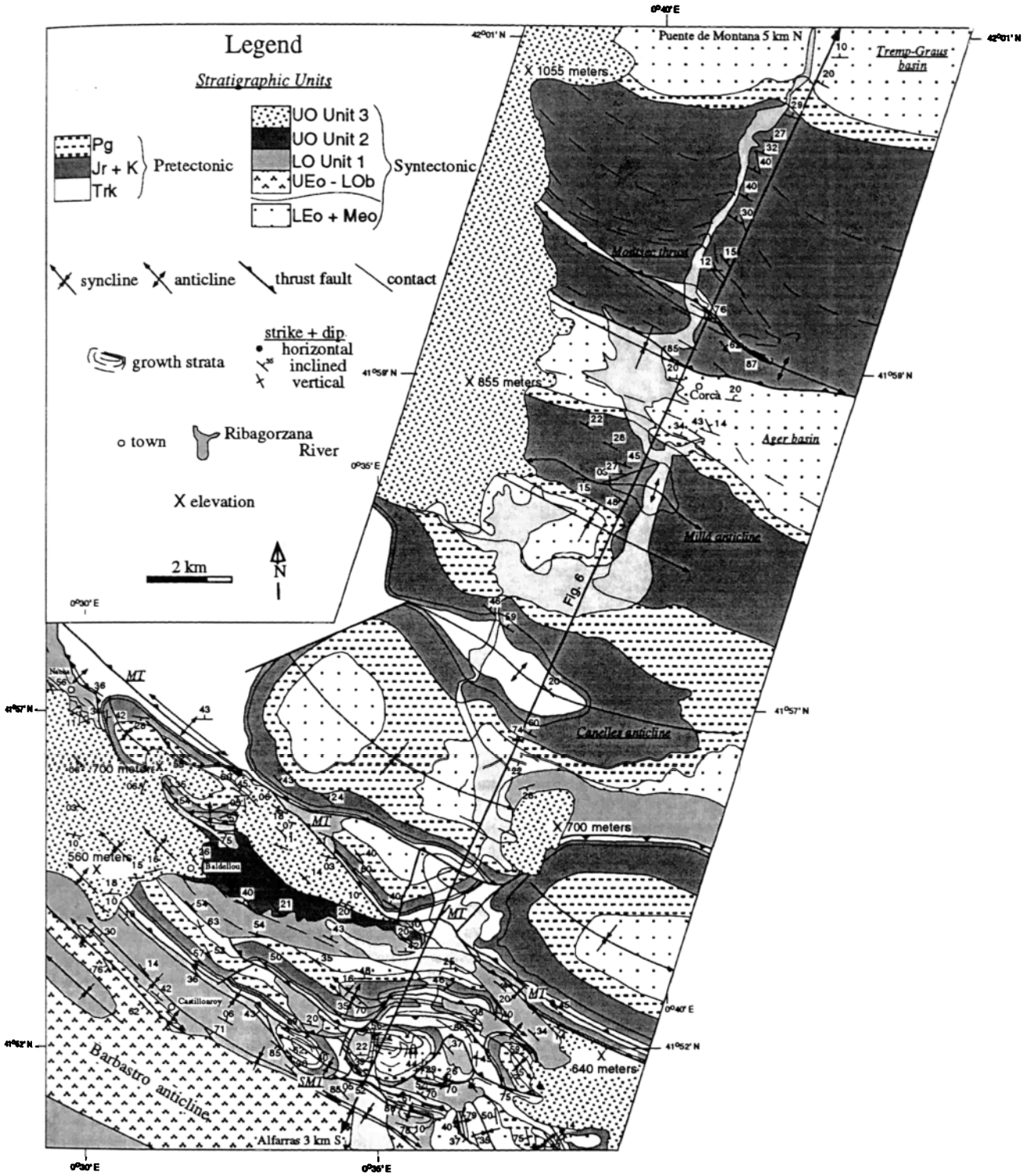

Figure 4. Geologic map of the study area. Compiled from extensive original field mapping, modifications of the map of *Pocoví* [1978a], and the geologic map of Catalunya [*Losantos et al.*, 1989]. The elevations of the highest points on the top of the youngest nonmarine syntectonic unit are denoted by crosses and the elevation in meters above sea level. SMT is the Sierras Marginales thrust and MT is the Montargull thrust. Stratigraphic units are subdivided into pretectonic and syntectonic groups. Pretectonic units are Trk, Triassic Keuper and Muschelkalk facies; Jr + K, Jurassic and Cretaceous carbonates undifferentiated; and Pg, Paleocene Garumnian facies. Syntectonic units are LEo + MEo, Lower and Middle Eocene limestones undifferentiated; UEo - LOb, Barbastro Formation; LO Unit 1, unit 1 in nonmarine strata; UO Unit 2, unit 2; and UO Unit 3, unit 3. Break between LEo + MEo and UEo - LOb marks the change from marine to nonmarine deposition in the syntectonic succession. The southern portion of the crustal section (Figure 6) is indicated.

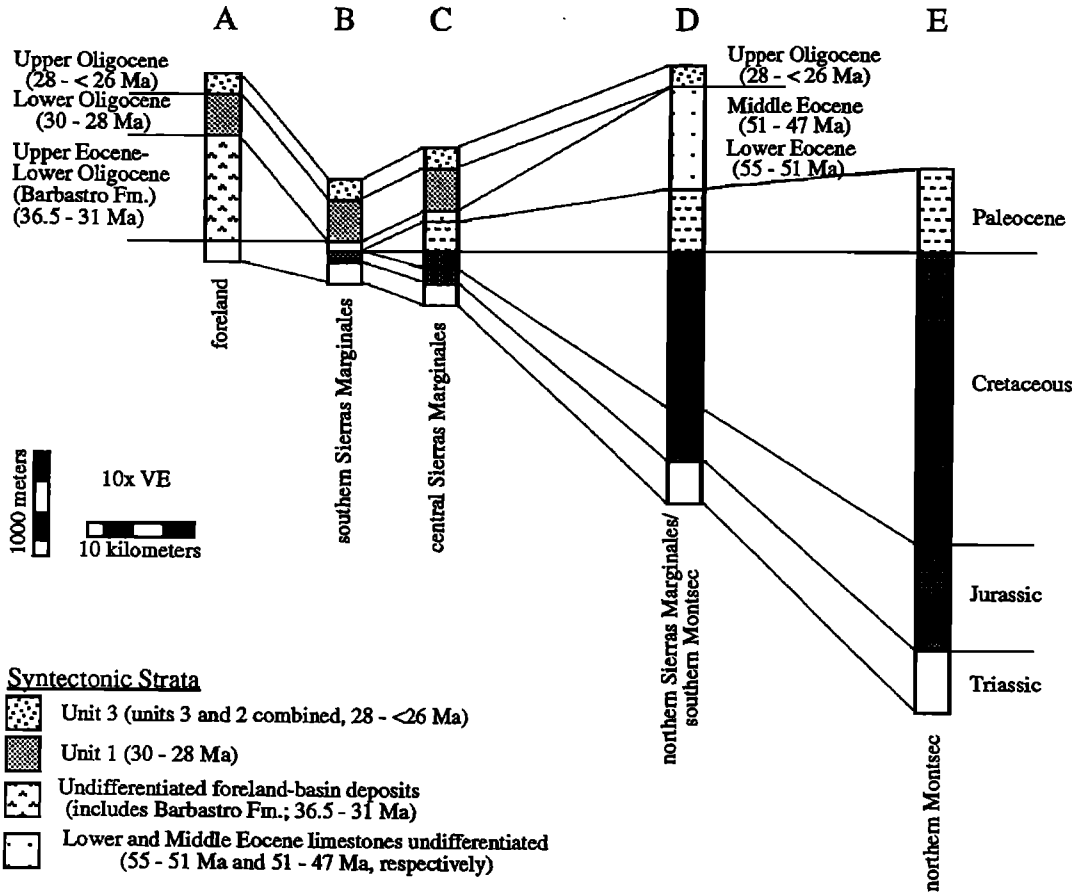

Figure 5. Stratigraphic columns for the study area. A northward thickening wedge of pretectonic strata (Triassic-Paleocene) is overlain by syntectonic strata (Eocene-Oligocene). Marine and terrestrial deposition characterize both pretectonic and syntectonic strata. Column A incorporates data from *Meigs* [1997] and *Senz and Zamorano* [1992]. Columns B and C were measured by *Pocoví* [1978a, b]. The Montsec sections are from *Simó and Puigdefàbregas* [1985] (columns D and E). Patterns are the same as Figure 4. See Figure 3 for localities A-E.

Stratigraphic Data

Stratigraphic information comes from a variety of sources. Measured sections and detailed stratigraphic analyses are abundant in the region. A study of an exposed part of the foreland basin succession to the west of the study area which integrated information from well logs and measured sections [*Senz and Zamorano*, 1992] and a measured section across a piggyback-basin succession within the study area were used to construct the stratigraphic column for the foreland (Figure 5A) [*Meigs*, 1997]. Thickness variations within the Sierras Marginales thrust sheet are known from a series of 14 measured sections (Figure 5, columns B and C) [*Pocoví*, 1978a, b). The greatest change in stratigraphic thickness within the Montsec thrust sheet is exhibited by Cretaceous rocks studied in detail by *Simó and Puigdefàbregas* [1985] (Figure 5, columns D and E). These stratigraphic data were combined with surficial structural information to constrain thickness on the cross sections.

A number of stratigraphic observations provide critical constraints on the spatial, temporal, and geometrical evolution of the thrust belt. The stratigraphy consists of rocks deposited prior to the onset of contractional deformation, pretectonic strata, and syntectonic rocks deposited coevally with folding and thrusting (Figures 5 and 7). Marine deposition on a north facing passive margin characterizes the Triassic through Cretaceous [*Pocoví* 1978a; *Simó and Puigdefàbregas*, 1985]. Lacustrine and fluvial rocks are preserved widely across the South-Central Unit and mark a short-lived interval of continental deposition in the Paleocene [*Pocoví*, 1978a; *Williams*, 1985]. Whereas these rocks are syntectonic with respect to the Bóixols thrust in the east (Figure 3), they are pretectonic with respect to the Montsec and Sierras Marginales thrust on the west [*Pocoví*, 1978a; *Williams*, 1985, *Muñoz*, 1992; *Puigdefàbregas et al.*, 1992; *Vergés*, 1993]. Because they are relatively thin, display only a gradual northward thickening, and are well exposed throughout the region, the Paleocene strata provide an ideal horizontal reference for stratigraphic and structural reconstructions [*Williams*, 1985; *Vergés*, 1993]. Overall, the pretectonic section thickens gradually from < 300 to 400 m on the south to > 5000 m on the north (Figure 5).

A return to marine sedimentation is coincident with the onset of contractional deformation in the study area (Figure 7) [*Pocoví*, 1978a; *Meigs and Burbank*, 1993; *Meigs*, 1997]. Syntectonic stratigraphic geometries observed in Lower Eocene marine limestones mark earliest-formed structures. Middle Eocene syntectonic strata consist of marine rocks on the south and

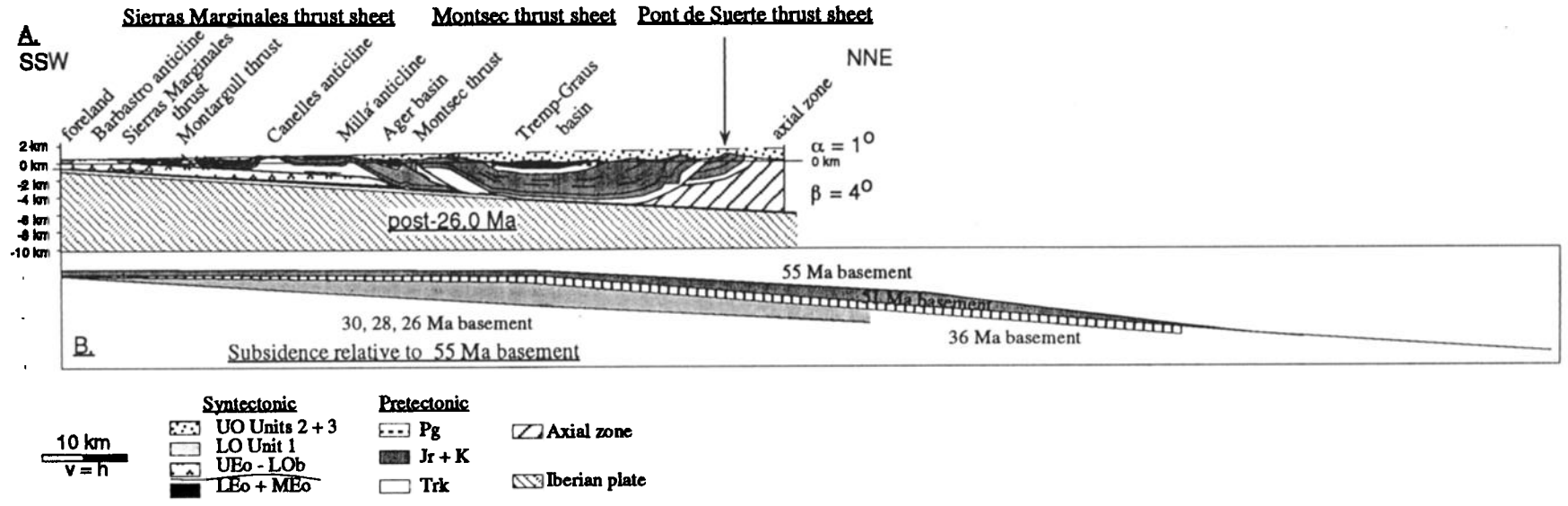

Figure 6. (a) Present-day geologic cross section (post-26 Ma) across the Pyrenean foreland fold-and-thrust belt parallel to the Ribagorzana River. From the southern edge of the Montsec thrust sheet to the north, the top of unit 3 is projected at the dip defined from observation from the Montsec southward (dashed line). The top is defined by the elevation of the highest exposure of the top of unit 3 on to the line of section (Figure 4). This projection is justified by the elevation of the top of slightly older, but similar, conglomerates in the northern portion of the study area (Figure 3) [*Losantos et al.*, 1989]. Topographic slope is 1.0°, and dip of the basal décollement is 4°. See text for discussion of data used in construction. (b) Plot of basement subsidence relative to 55 Ma basement. Note that the position of the basement is inferred to have remained approximately fixed after 30 Ma. See text for discussion. See Figures 3 and 4 for location. See *Meigs* [1997] for detailed analysis of southern edge of Sierras Marginales thrust sheet. Except for Lower and Middle Eocene syntectonic strata patterned black, the patterns and stratigraphic units are the same as Figure 4. Pretectonic units are Trk, Triassic Keuper and Muschelkalk facies; Jr + K, Jurassic and Cretaceous carbonates undifferentiated; and Pg, Paleocene Garumnian facies. Syntectonic units are LEo + MEo, Lower and Middle Eocene limestones undifferentiated; UEo - LOb, Barbastro Formation; LO Unit 1, unit 1 in nonmarine strata; UO Unit 2, unit 2; and UO Unit 3, unit 3.

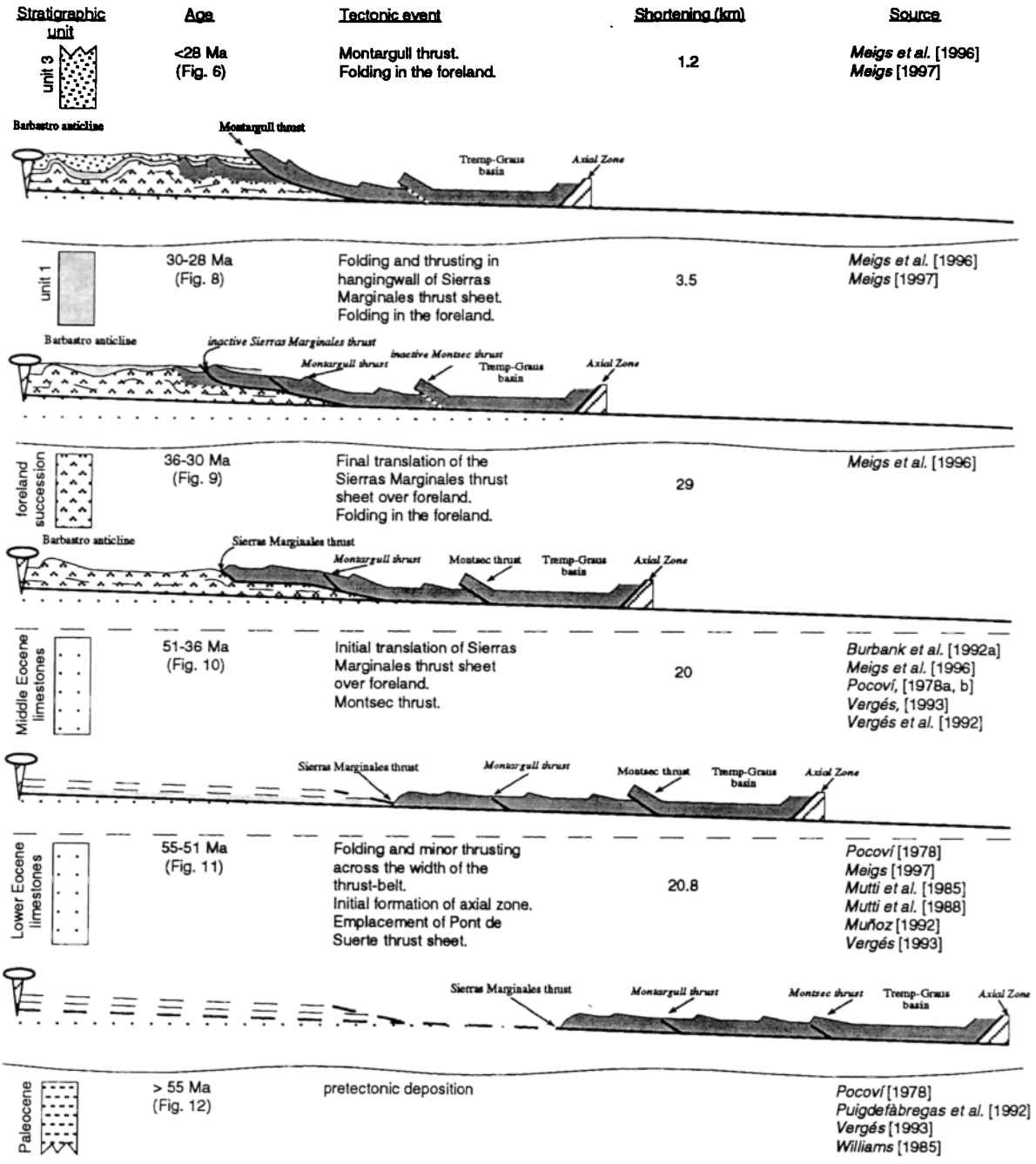

Figure 7. Summary diagram of syntectonic stratigraphic units, ages, tectonic events occurring contemporaneously with deposition of each distinct unit, and data source. Note that the figure of the corresponding structural cross section is indicated in parentheses below the age. Dashed lines represent inferred or known conformable contacts. Wavy lines represent mapped unconformities (see Figure 4). Total shortening measured for a given interval is given in kilometers. See text for complete descriptions of the tectonic events. Structural development sketches are approximately scaled horizontally and have no implied vertical scale. Coeval deposition is schematically depicted in the foreland but not in piggyback basins developed on the thrust belt.

transitional to nonmarine rocks on the north [*Pocoví*, 1978a; *Mutti et al.*, 1985, *Puigdefàbregas et al.*, 1992; *Vergés et al.*, 1992; *Vergés*, 1993]. Because Lower and Middle Eocene rocks are characterized by shallow marine and shallow interfingering with nonmarine facies, respectively [*Pocoví*, 1978a; *Mutti et al.*, 1985; *Mutti et al.*, 1988], they constrain the position of the thrust belt's upper surface with respect to sea level during the early stages of development. Finally, Upper Eocene through Oligocene nonmarine sediments in the Ebro foreland basin and in piggyback basins on top of the evolving thrust belt constrain depth of fill,

extent of burial of structures, paleorelief on basin-margin structures, and synorogenic topography during later stages of contractional deformation [*Burbank et al.*, 1992b; *Vergés*, 1993; *Burbank and Vergés*, 1994; *Meigs et al.*, 1996; *Meigs*, 1997]. Present stratigraphic thickness were used and no attempt was made to decompact the syntectonic strata.

Subsurface Data

Although no subsurface data were available within the study area, a wide range of subsurface information has been published throughout the region. Several major questions regarding the deep crustal structure of the Pyrenees were resolved after the acquisition and interpretation of the ECORS deep seismic profile (Figure 3) [*Choukroune and ECORS Team*, 1989; *Muñoz*, 1992; *Roure et al.*, 1989]. This seismic line clearly imaged the basal décollement of the Pyrenees and constrained its depth and nearly constant dip northward to beneath the axial zone [*Muñoz*, 1992]. The exact dip and depth are somewhat variable along strike (3.5° -4°; [*Muñoz*, 1992; *Vergés*, 1993]). Therefore stratigraphic data within the study area, a crustal section to the west [*Senz and Zamorano*, 1992], and a well-constrained grid of detailed balanced cross sections constructed to the east [*Vergés*, 1993] were used to constrain the present dip as ~4° +/- 0.5° at a depth of -1000 m on the south beneath the foreland to -4500 m below the Tremp-Graus basin on the north (Figure 6).

A number of other important subsurface structures, which have no obvious surface expression in the study area but that are assumed to exist at depth and are included in the geologic section, were revealed by the ECORS project and subsequent studies (Figure 6). A footwall anticline beneath the Montsec thrust fault was penetrated by the Comiols well (Figure 3), is seen on the ECORS section, and is inferred to exist along the strike length of the fault [*Muñoz*, 1992; *Vergés*, 1993]. Although the Sierras Marginales thrust was previously suspected to be significantly displaced with respect to its footwall cutoff [*Martínez Peña and Pocoví*, 1988], the position of the cutoff was unconstrained prior to the ECORS profile. Given the ECORS image [*Muñoz*, 1992] and subsequent structural, stratigraphic, and paleogeographic reconstructions [*Vergés*, 1993], the displacement of the Sierras Marginales thrust sheet is well constrained regionally as ~45 m. A comparable amount of displacement is inferred in this study.

A final debate, spawned in part by the ECORS results, concerns the nature of the rocks sandwiched between the base of the Sierras Marginales thrust sheet and the basal décollement. *Muñoz* [1992] argued on the basis of structural relationships near the southern edge of the sheet that this subsurface space was filled by a "double" Sierras Marginales, a complete thrust duplication of the sheet. On the basis of structural, stratigraphic, and subsurface data, in contrast, subsequent authors argued that the Sierras Marginales thrust sheet had translated over a significant portion of the foreland [*Senz and Zamorano*, 1992; *Vergés et al.*, 1992; *Vergés*, 1993; *Meigs et al.*, 1996]. Because substantial duplication of the Sierras Marginales thrust sheet is only locally observed in the study area [*Meigs*, 1997], the Sierras Marginales thrust sheet is interpreted to have been displaced over the foreland (Figure 6). The position of the ramp across the foreland is inferred to sit below the south flank of the Ager basin, an interpretation supported by surface dip data and consistent with other analyses [*Senz and Zamorano*, 1992; *Vergés*, 1993].

Age Data

Absolute ages of deformational periods come exclusively from Lower Eocene to Oligocene syntectonic sediments dated biostratigraphically and magnetostratigraphically (Figure 7). No thermochronologic age data was available for the area. Upper Eocene and Oligocene nonmarine deposits have been dated paleomagnetically [*Meigs et al.*, 1996; *Meigs*, 1997]. In addition to the deformational chronology in the study area [*Meigs*, 1997], a chronology determined along strike to the east at Artesa de Segre (Figure 3) is incorporated because it contains a similar record of deformation to that of the study area and clear evidence of older deformation in addition [*Meigs et al.*, 1996]. Lower and Middle Eocene marine rocks have been dated biostratigraphically [*Pocoví*, 1978a, b; *Williams and Fischer*, 1984; *Mutti et al.*, 1985, 1988; *Farrell et al.*, 1987; *Muñoz*, 1992; *Puigdefàbregas et al.*, 1992]. Six distinct stages in the development of the Pyrenean foreland fold-and-thrust belt can be differentiated with confidence based on syntectonic sediments and structural relationships. Sequential restoration of the present cross section (Figure 6) reveals the thrust belt geometry as the effects of deformation after 28.0 Ma (Figure 8), between 28 and 30 Ma (Figure 9), between 30 and 36 Ma (Figure 10), between 36 and 51 Ma (Figure 11), and between 51 and 55 Ma (Figure 12) are stripped away.

The most recent deformation affected the youngest exposed syntectonic sediments on a few structures in the study area, but these strata are otherwise undeformed and unconformably overlie nearly every structure (Figures 4 and 6). These nonmarine alluvial and fluvial rocks are informally referred to as unit 3, which includes, for the purposes of this study, a distinct locally exposed and preserved conglomeratic unit (unit 2 [*Meigs*, 1997]). Unit 3 ranges in age from 27.9 to < 25.8 Ma. A lithologically similar deposit occupying an analogous structural and stratigraphic position at Artesa de Segre ranges in age from 27.8 to < 24.6 Ma [*Meigs et al.*, 1996]. Deformation affecting unit 3 occurred after 28.0 Ma.

Deformation between 30 and 28 Ma is marked by folding and thrusting of unit 1 (Figures 4, 5, and 7). Unit 1 unconformably overlies a variety of older rocks on both the Sierras Marginales thrust sheet and in the foreland [*Meigs et al.*, 1996]. It is unconformably overlain by unit 3. In contrast to unit 3, unit 1 is deformed everywhere it is exposed (Figure 4). Unit 1 ranges in age from 30.1 to 28.0 Ma [*Meigs*, 1997]. Unit 1 also has a structurally and stratigraphically correlative unit at Artesa de Segre that ranges in age from 29.5 to 28.5 Ma [*Meigs et al.*, 1996]. Growth stratal geometries in unit 1 indicate that the deformation occurred coevally with deposition.

The third deformational episode (36 to 30 Ma) is tightly constrained by relationships at Artesa de Segre [*Vergés*, 1993; *Vergés et al.*, 1992; *Meigs et al.*, 1996]. Map relationships suggest that the Sierras Marginales thrust sheet was emplaced across previously folded foreland basin strata. Both the Sierras Marginales thrust and folded foreland sequence are unconformably overlain by unit 1. The exposed portion of the foreland-basin succession at Artesa ranges in age from 36.5 to 30.7 Ma. This unconformable relationship indicates that the Sierras Marginales thrust sheet was in its present position by ~30 Ma. A combination of geometrical observations, subsurface relationships, and paleogeographic interpretations support the inference that the Sierras Marginales thrust sheet began to override the foreland succession at ~36.5 Ma.

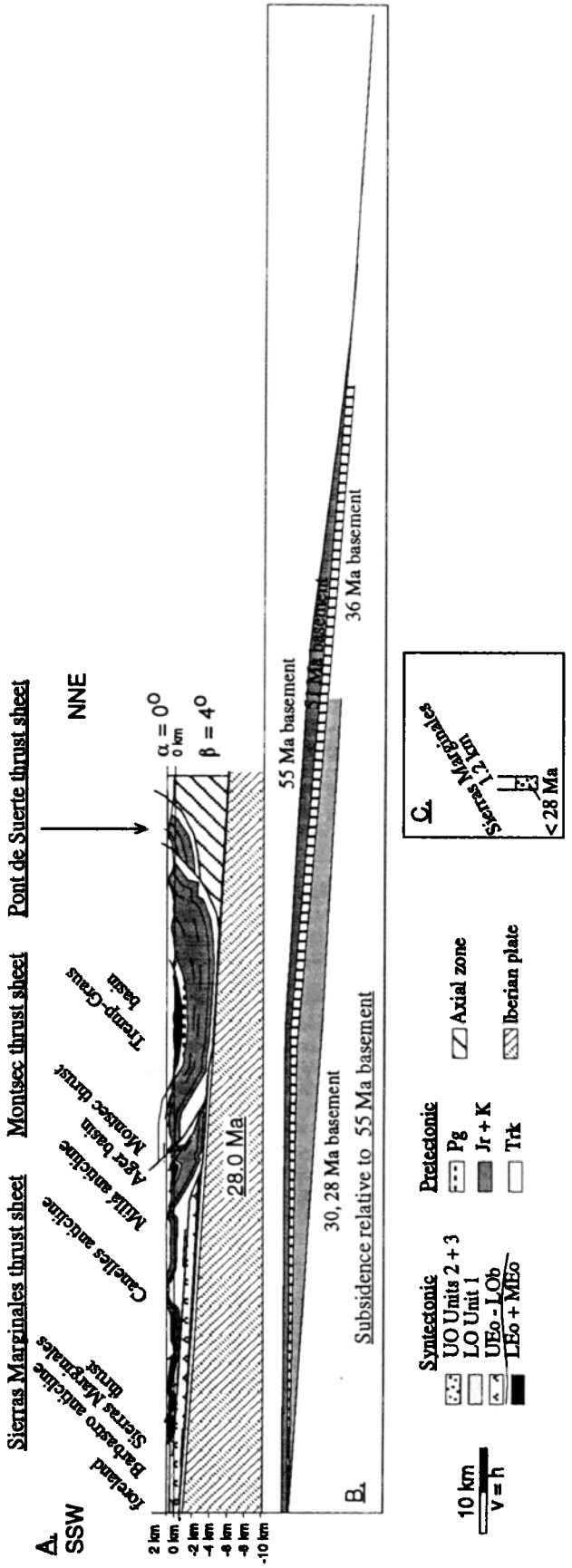

A poorly constrained period of shortening between 51 and 36 Ma is inferred for the study area based on deformational events elsewhere in the Pyrenees during the same period. Within the study area, Middle Eocene (Lutetian) limestones that unconformably overlie tilted older strata are themselves folded and unconformably overlain by unit 1 [*Pocoví*, 1978a, b; *Meigs*, 1997]. Middle Eocene strata are present in the footwall of the Sierras Marginales thrust sheet (beneath the Ager basin and Montsec thrust, Figure 6). Well-constrained Middle Eocene shortening on the structurally correlative thrust sheet of the Sierras Marginales thrust sheet in the eastern Pyrenees, the lower Pedraforca thrust sheet [*Martínez et al.*, 1988; *Burbank et al.*, 1992a; *Vergés et al.*, 1992, 1995; *Vergés*, 1993], implies contemporaneous shortening in the South-Central Unit. On this basis, we differentiate a discrete deformational period between ~51 Ma and 36 Ma.

Initial shortening in the study area is marked by growth stratal geometries [*Riba*, 1976; *Anadón et al.*, 1986; *Vergés et al.*, 1996] in Lower Eocene marine limestones [*Meigs*, 1997]. Well-constrained biostratigraphically determined ages of these limestones place the initial deformation in the Early Ypresian (55 to 51 Ma [*Pocoví*, 1978a; *Mutti et al.*, 1985, 1988; *Cande and Kent*, 1992; *Muñoz*, 1992; *Vergés*, 1993]). Restoration of this deformation defines the pre-55-Ma geometry of the pretectonic stratigraphic wedge.

When combined with stratal thickness and structural geometries, these constraints allow sequential restoration of the dip of the basal décollement, the topographic surface, and the internal structural geometry of the Pyrenean thrust belt from its present, postdeformational state backward through time to its predeformational state in five distinct temporal steps.

Six Steps in the Evolution of the Pyrenean Wedge

A deformed state cross section is an aggregate of superposed deformations [*Geiser*, 1988; *Meigs*, 1997]. Sequential restoration is a process of tectonic "backstripping" which, through the restoration of structures resulting from an individual period deformation, reveals the consequences of successive deformations. The Pyrenean foreland fold-and-thrust belt is stepped backward through time from its present cross-sectional geometry to its predeformational geometry in four intermediate steps (Figures 6 and 8-12). Each restoration involves the removal of shortening accommodated by displacement on faults and/or by folding as recorded by the relationship between folds and faults and syntectonic strata [*DeCelles et al.*, 1991; *Vergés et al.*, 1996; *Meigs*, 1997]. Details of the restoration procedure and geometrical justification for structures on the southern edge of the Sierras Marginales thrust sheet are given by *Meigs* [1997]. In

Figure 8. 28.0-Ma reconstruction. (a) Total recovered shortening is 1.2 km from reconstruction of a fold in the former position of the Montargull thrust (Figure 6). Topographic slope is 0° and dip of the basal décollement is 4°. (b) Plot of basement subsidence relative to 55 Ma basement. Note that the position of the basement is inferred to have remained approximately fixed after 30 Ma. See text for discussion. (c) Shortening recovered from restoration of structures active after 28 Ma. Patterns and stratigraphic units are the same as Figure 6.

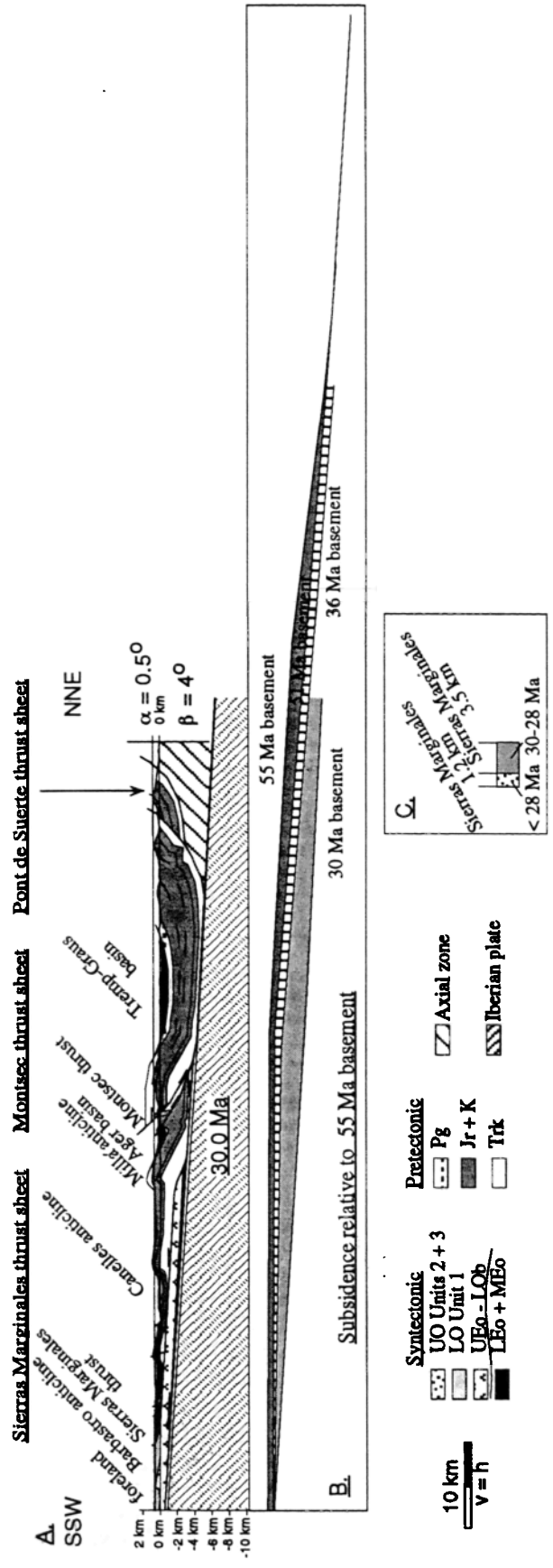

addition, the tectonic subsidence of the basement is recovered by "hanging" partial restorations of the deformed state cross section constrained stratigraphically and structurally.

Line length and area are conserved between each step for the pretectonic strata and Triassic evaporites, respectively. Shortening is measured by the change in position of a pin line located in the axial zone with respect to a pin line in the undeformed foreland on the south of the section. The hinterland pin line has no geological significance, it merely serves as a reference with which the forelandward displacement of the rear of the deforming wedge can be measured. Because of uncertainty in fault displacements where hanging wall cutoffs are eroded and shortening related to undocumented fabrics, such as cleavage, formed by layer-parallel shortening, intermediate and total shortening estimates are minimum values. Such reconstructions illustrate the evolution of internal deformation and emplacement of the thrust belt. Structural relief and stratigraphic relationships allow approximation of topography for each step. In particular, the preserved thickness of syntectonic strata are used to constrain the upper surface of the wedge at each step.

Present (Post-28-Ma) Cross Section

The present-day cross section (Figure 6) reflects the geometry of the thrust belt after 28 Ma, after the final deformational pulse [*Meigs*, 1997]. Nearly every structure is buried by the youngest nonmarine clastic deposit (unit 3) whose age ranges from 27.9 to < 25.8 Ma (Figures 4 and 6). Unit 1 is deformed by the Montargull thrust and related imbricates and probably by late modification of the Barbastro anticline in the foreland (Figure 7). A cross-sectional taper of 5° is given by the 4°-dip basal detachment and 1°-slope of the top of unit 3 (Figure 6). This surface is constrained from the hanging wall of the Montsec thrust to the foreland by projection of the highest exposures of unit 3 along strike onto the line of the section (Figure 4). This surface is only a "best guess" of topography because the age of the highest unit at any spot is likely to be diachronous. Tight limits on possible uncertainty in the angle of the surface slope (+/- << 0.5°) are indicated to the south of the Montsec because unit 3 barely overtops structural highs that otherwise would define the surface slope. The projection to the north of the Montsec is an extrapolation of the average slope defined to the south (dashed line, Figure 6). Its elevation and thickness are consistent with nonmarine alluvial and fluvial deposits (Collegats Formation) that discontinuously overlie the contact between the axial zone and the rear of the foreland fold-and-thrust belt [*Mellere*, 1992, 1993; *Vergés*, 1993]. Note that the depth-to-basement and angle of the basement are the same after 30 Ma

Figure 9. 30.0-Ma reconstruction. (a) Restoration of nearly all thrust faults within the Sierras Marginales thrust sheet accounts for 3.5 km of shortening, and the Montsec thrust and related imbricates are associated with 5 km of shortening. Topographic slope is 0.5° and dip of the basal décollement is 4°. (b) Plot of basement subsidence relative to 55° Ma basement. Note that significant basement subsidence is inferred to have occurred between 36 and 30 Ma. See text for discussion. (c) Shortening recovered from restoration of structures active after 28 Ma and between 28 and 30 Ma. Patterns and stratigraphic units are the same as Figure 6.

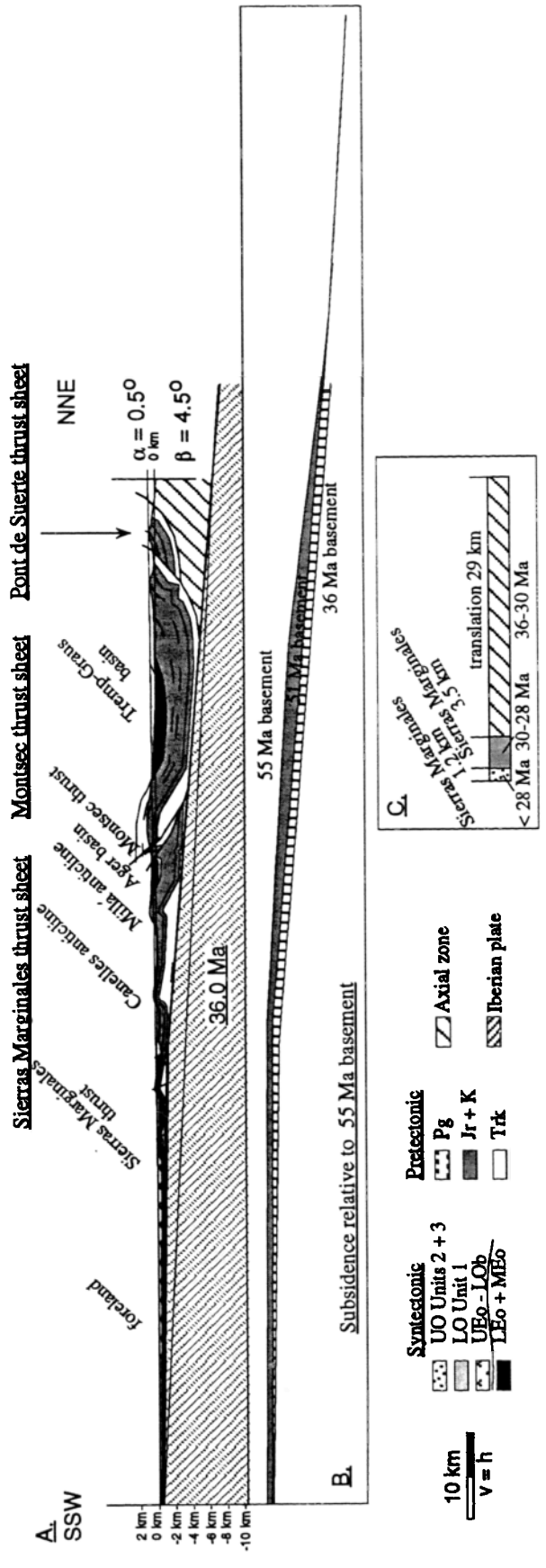

(Figures 6, 8, and 9). Although 0.5-1 km of material have been removed from above the Tremp-Graus basin since 28 Ma (Figure 6), the taper is based on structural and rock thicknesses. Erosional removal of this material and consequent rebound would change both the basal décollement and surface slope angles, but the total taper would remain the same.

28-Ma Cross Section

Removal of unit 3 and restoration of structures that deform it defines the 28 Ma cross section (Figure 8). Structures remaining in the section reflect shortening prior to 28 Ma. Unit 3 has been stripped off the section, a fold has been reconstructed in the former site of the Montargull thrust, and a minor amount of shortening is removed from the Barbastro anticline [*Meigs et al.*, 1996; *Meigs*, 1997], otherwise the section is the same as in the previous cross section. Restoration of these structures recovers 1.2 km of shortening. Note that the dip of the basal detachment, 4°, would have changed only if significant thickening in the Tremp Graus basin or shortening to the south had occurred. No evidence exists for this deformation. The 0° topographic slope is approximated by connecting a line from the highest structural relief on the north end of the section with the foreland. A wedge taper of 4° is indicated. This represents a minimum angle given uncertainty in the synorogenic relief on the Montsec hanging wall or the Millá and Canelles anticlines. Whereas the crests of the remaining anticlines project both above and below this line, the top of unit 1 lies entirely below. We assume, conservatively, that the eroded crest of these structures reflects crestal erosion that occurred during formation of the fold. It is inferred that the rate of erosion was less than the rate of uplift because resistant strata are exposed on the flanks at the surface and because of their present structural relief [*DeCelles et al.*, 1991; *Hogan*, 1993; *Burbank and Vergés*, 1994; *DeCelles and Mitra*, 1995].

30-Ma Cross Section

Folding and faulting of unit 1 resulted from a modest amount of shortening on the southern edge, in the hanging wall, of the Sierras Marginales thrust sheet between 30 and 28 Ma [*Meigs*, 1997]; the effects of this deformation must be removed to construct the 30.0 Ma cross section (Figure 9). Also recovered is a minor amount of shortening related to the Barbastro, Canelles, and Millá anticlines. Unit 1 unconformably overlies the southern flank of the Canelles anticline and is folded (Figure 4). The Millá anticline is interpreted to have been slightly modified during its

Figure 10. 36.0-Ma reconstruction. (a) Restoration of translation of the Sierras Marginales thrust sheet and minor folding in the foreland. and the geometry of the thrust belt just after activation of the detachment at the base and accretion of the foreland-basin succession is depicted. Topographic slope is 0.5°. Average dip of the basal décollement is 3° but consists, in detail, of a 4.5°-reach beneath the deformed thrust belt and a 1°-reach beneath the undeformed foreland. (b) Plot of basement subsidence relative to 55 Ma basement. Note that only a moderate amount of basement subsidence is inferred to have occurred between 51 and 36 Ma. See text for discussion. (c) Shortening recovered from restoration of structures active after 28 Ma, between 28 and 30 Ma, and between 30 and 36 Ma. Patterns and stratigraphic units are the same as Figure 6.

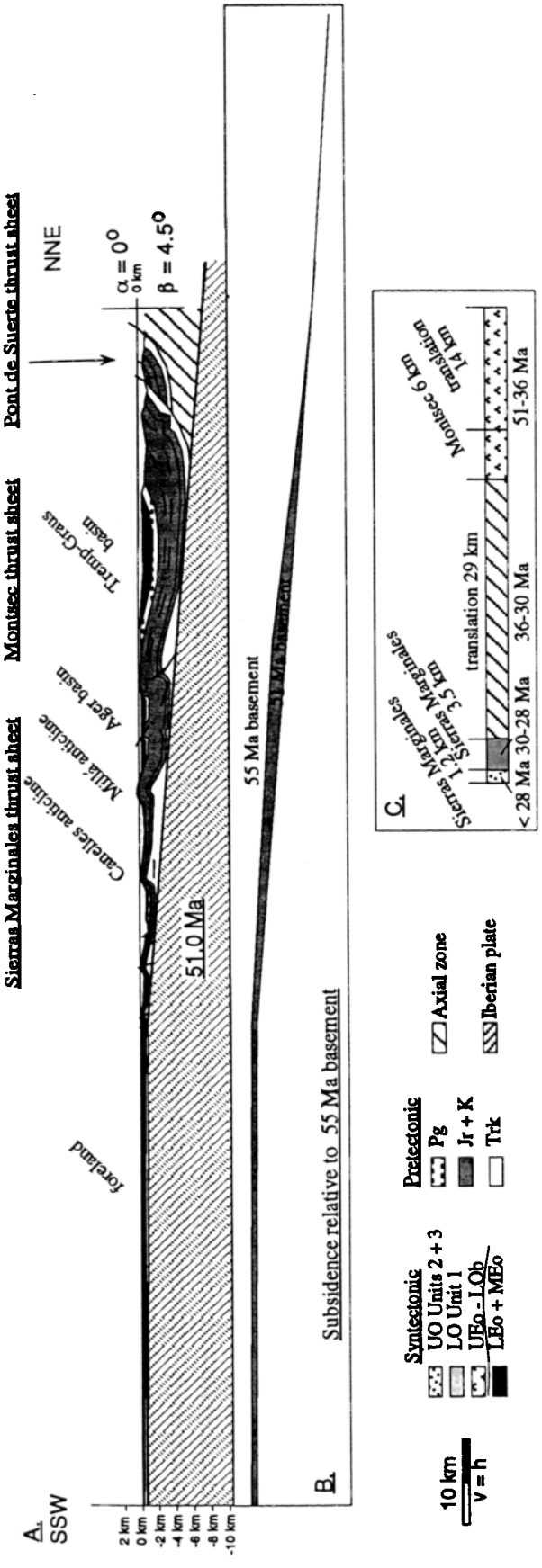

passage over the footwall ramp cutting the foreland-basin sequence in the subsurface. A total of 3.5 km of shortening is related to structures that deform unit 1. The dip of the basal detachment remained constant at 4°. Because structural relief created by folds and faults at the leading edge of the Sierras Marginales thrust sheet was less than the differential relief produced by displacement of the rear of the wedge up the basal décollement between 30 and 28 Ma, a positive slope to the topographic surface (0.5°) is reconstructed (Figure 9).

36-Ma Cross Section

Most of the shortening that remains within the partially restored section at 30 Ma accumulated between 51 and 30 Ma as a consequence of emplacement of the Sierras Marginales thrust sheet (Figures 9, 10, and 11) [*Martínez Peña and Pocoví*, 1988; *Muñoz*, 1992; *Vergés*, 1993; *Meigs et al.*, 1996]. Translation of the Sierras Marginales thrust sheet occurred in two discrete stages (Figure 7): (1) an initial 14-km translation from its footwall cutoff to approximately the base of a footwall ramp across the foreland-basin sequence between 51 and 36 Ma (Figures 10 and 11) [*Muñoz*, 1992; *Vergés*, 1993; *Vergés et al.*, 1992] and (2) a 29-km translation to its present position across the foreland-basin sequence between 36 and 30 Ma (Figures 9 and 10) [*Meigs et al.*, 1996].

Map, stratigraphic, and geometrical relationships suggest that translation of the Sierras Marginales thrust sheet (and, by extension, piggy back translation of the entire thrust belt) over the foreland-basin succession occurred after 36 Ma and was complete by 29.5 Ma [*Meigs et al.*, 1996]. Early folding of the foreland-basin succession is also recovered in the 36 Ma restoration (Figure 10). Initiation of slip on the segment of the basal décollement at the base of the foreland-basin succession occurred at ~ 36.5 Ma over a broad region of the thrust belt (Oliana [*Burbank et al.*, 1992b]; Artesa de Segre [*Meigs et al.*, 1996], Figure 3) and was coincident with initial displacement of the Sierras Marginales across the foreland [*Meigs et al.*, 1996]. Given the geometrical resolution of the stratigraphic data, no internal deformation within the thrust belt is recognized between 36 and 30 Ma.

Topography developed between 51 and 36 Ma was influenced primarily by displacement on the Montsec thrust and translation of the thick stratigraphic section at the rear of wedge up the basal décollement (Figures 10 and 11). A surface slope of 0.5° is indicated for this restoration. An average surface slope lower

Figure 11. 51.0-Ma reconstruction. (a) The stratigraphic wedge is foreshortened 2.8 km by a series of folds whose amplitude and spacing decrease to the south. Note 18.0 km of shortening between the axial zone and Pont de Suerte thrust sheet and the thrust belt. Note also that the top of the wedge is at sea level. Topographic slope is 0° and dip of the basal décollement is 4.5°. (b) Plot of basement subsidence relative to 55 Ma basement. Note that because the topographic slope is 0°, the wedge taper is a reflection of basement subsidence driven by tectonic loading between 51 and 55 Ma. See text for discussion. (c) Shortening recovered from restoration of structures active after 28 Ma, between 28 and 30 Ma, between 30 and 36 Ma, and between 36 and 51 Ma. Patterns and stratigraphic units are the same as Figure 6.

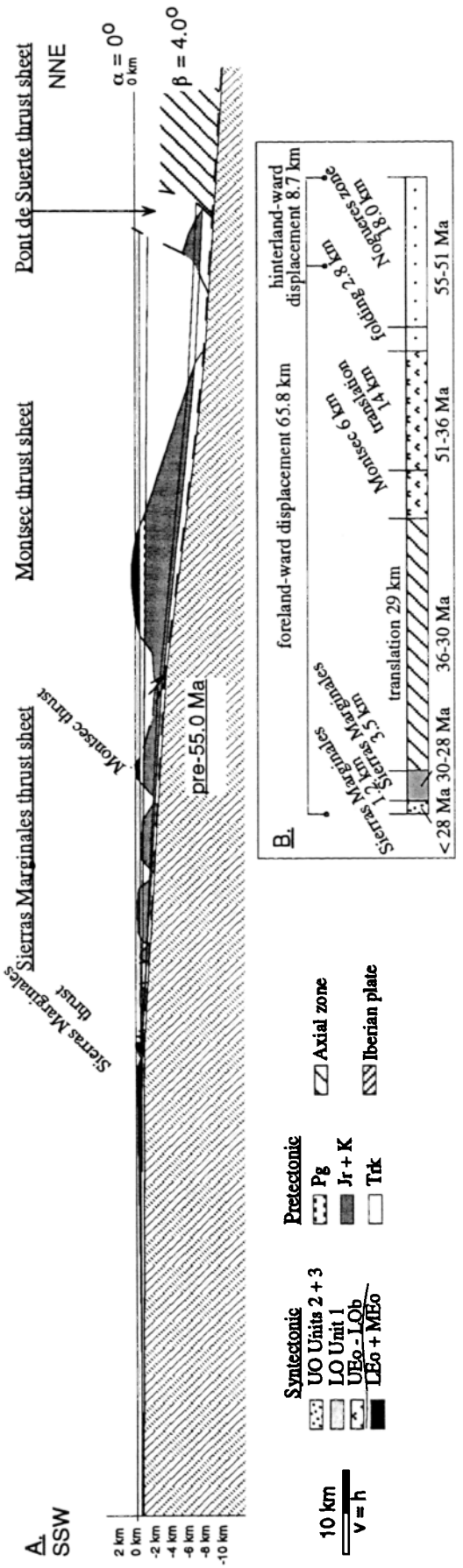

Figure 12. Pre-55.0-Ma reconstruction, a total restoration of figure 6. A) A total of 65.8 km of forelandward translation of slip is recovered by restoring all major structures. Displacement of the axial zone wedge with respect to the rear of the thrust belt includes ~7 km of backthrust (to the north) displacement. The stratigraphic taper is 4°. (b) Shortening recovered from restoration of structures active after 28 Ma, between 28 and 30 Ma, between 30 and 36 Ma, between 36 and 51 Ma, and between 51 and 55 Ma. Patterns and stratigraphic units are the same as Figure 6.

than 0.5° is unlikely given that the basin-bounding structures of the Ager and Tremp piggyback basins were probably emergent above the Middle Eocene depositional surface (Figures 4 and 10). Middle Eocene strata onlap the flanks and are structurally and topographically lower than the crests of adjacent basin-bounding structures. The basal décollement dip at 36 Ma (3.0°) is defined by a line connecting the base of the rear of the wedge with the thrust tip (Figure 10). Clearly, this is an average dip and does not reflect the fact that the geometry of the basal décollement at the instant of accretion consists of two domains: (1) a 4.5° domain beneath the deformed wedge developed after deformation between 55 and 36 Ma and (2) a 1° domain beneath the accreted, but as yet undeformed, foreland-basin material.

51-Ma Cross Section

The 51 Ma cross section reflects restoration of shortening due to approximately 6 kms of displacement on the Montsec thrust and initial displacement of the Sierras Marginales thrust sheet from its footwall cutoff to its 36 Ma position at the base of the ramp across the foreland-basin succession (Figures 10 and 11). Folding and thrust displacement associated with the Montsec thrust and related imbricates began after 55 Ma and continued until 33.5 Ma [*Williams and Fischer*, 1984; *Williams*, 1985; *Burbank et al.*, 1992b; *Muñoz*, 1992; *Vergés*, 1993]. Because Ypresian (55-51 Ma [*Cande and Kent*, 1992]) growth strata deposited on the limbs of a fold now cut by the Montsec thrust (Figures 4 and 10) [*Misch*, 1934; *Mutti et al.*, 1985, 1988; *Martínez Peña and Pocoví*, 1988], thrust displacement is inferred to have occurred after initial folding between 55 and 51 Ma but before 36 Ma. Palinspastic restoration of the structurally correlative thrust sheet in the eastern Pyrenees, constrained by syntectonic strata, implies a ~12 km translation of the Sierras Marginales thrust sheet between 51 and 36 Ma [*Burbank et al.*, 1992b; *Vergés et al.*, 1992; *Vergés*, 1993] Fourteen kilometers are estimated for this line of section (Figure 11).

Distributed deformation across the width of the thrust belt from 55 to 51 Ma is indicated by growth-stratal geometries in Lower Eocene marine strata deposited in a series of piggy back basins preserved within the thrust belt [*Pocoví*, 1978a, b; *Mutti et al.*, 1985, 1988; *Meigs*, 1997]. These strata demonstrate that folds in the future site of the Montsec thrust and related imbricates, the Millá and Canelles anticlines, and two smaller folds near the leading edge of the Sierras Marginales thrust sheet developed at this time. Both the Tremp-Graus basin and the rear of the wedge are treated as fixed by 51 Ma and carried forward in time unmodified. This is significant because the thickness in the center of the Tremp-Graus basin and the structural relief represented by its north flank influence significantly

reconstruction of the surface slope in subsequent restorations. A minor amount of deformation on the north flank of the basin that caused slight modification of the rear of the wedge until the Early Oligocene [*Mellere*, 1993] is not incorporated into successively younger sections (Figures 10, 9, 8, and 6). For the 51 Ma restoration (Figure 11), a combination of internal structural thickening and using the top of Lower Eocene rocks to approximate paleo sea level, (an inference supported by the observation that the Lower Eocene is dominated by shallow marine facies [*Pocoví*, 1978a, b; *Mutti et al.*, 1985, 1988] allows a 0° topographic slope and 4.5° basal décollement angle at 51 Ma to be inferred.

Totally Restored (Pre-55-Ma) Cross Section

The pre-55-Ma cross section is a full restoration of the post-28.0-Ma cross section (Figures 6 and 12). Paleocene rocks, comprising continental alluvial and lacustrine strata, serve as a horizontal datum for restoration of the stratigraphic units because of their widespread preservation over the South-Central Unit (Figure 4) [*Williams*, 1985; *Puigdefàbregas et al.*, 1992; *Vergés*, 1993]. Approximately 20.8 km of shortening remained in the 51-Ma section (Figure 11): 2.8 km are due to folding within the foreland fold-and-thrust belt and 18.0 km are due to displacement of the axial zone wedge beneath the rear of the thrust-belt (Figure 12). The restored position of the Pont De Suerte thrust sheet is dictated by the restored area of Triassic strata. A 4° taper of pre-Paleocene rocks results from this restoration. The total restored shortening of the internal structures is 75.5 km, whereas the total forelandward displacement of the trailing pin line is 68.8 km. This suggests that backthrust displacement, toward the hinterland, across the fault separating the foreland thrust-belt from the crystalline core is ~6.7 km. Structural geometries are highly simplified on the north end of the section, so these values should be considered only a rough estimate of the actual value of displacement. A limited amount of backthrust displacement across this fault is more consistent with crustal interpretations in which the total shortening in the axial zone is nearly balanced by that in the foreland fold-and-thrust belt [*Vergés*, 1993; *Vergés et al.*, 1995] than interpretations in which shortening in the axial zone is greater than in the thrust belt [*Muñoz*, 1992].

The age of formation of the axial zone is not well constrained. From structural considerations alone, restoration of the rear of the wedge in this interval is reasonable if shortening in the axial zone antiformal-stack duplex is coupled to shortening in the foreland because the structurally highest and oldest horse of the duplex, the Nougats thrust sheet, lies directly beneath the trailing edge of the foreland fold-and-thrust belt [*Williams and Fischer*, 1984; *Williams*, 1985; *Muñoz*, 1992; *Vergés*, 1993; *Vergés et al.*, 1996]. Conglomerates deposited over the fault between the axial zone and trailing edge of the thrust belt are Upper Eocene to lowermost Oligocene, suggesting emplacement of the highest horses of the duplex before ~34 Ma [*Mellere*, 1992, 1993; *Sudre et al.*, 1992].

Thrust-Front Advance, Internal Deformation, and Taper Evolution of the Pyrenees

Comparison of the amount and style of thrust-front advance, internal deformation, and taper of the thrust belt through time is illustrative (Figure 13). Before the onset of contraction, a 4° stratigraphic taper is given by the complete restoration of the geologic cross section (Figure 12). At ~ 55 Ma, the thrust front propagated ~100 km to the south, and internal deformation initiated by folding across the width of the thrust belt (Figures 11 and 13). Because the surface of the thrust belt was at or near sea level between 55 and 51 Ma (Figures 13 and 14), we use the top of marine strata deposited at this time as a proxy for sea level to infer a 0° surface slope for the wedge at this stage. The taper-angle change from 4° at 55 Ma to 4.5° at 51 Ma therefore resulted from tectonic subsidence of the basement as a consequence, primarily, of initial formation of the axial zone in the hinterland and, secondarily, from internal deformation (Figure 11b). A

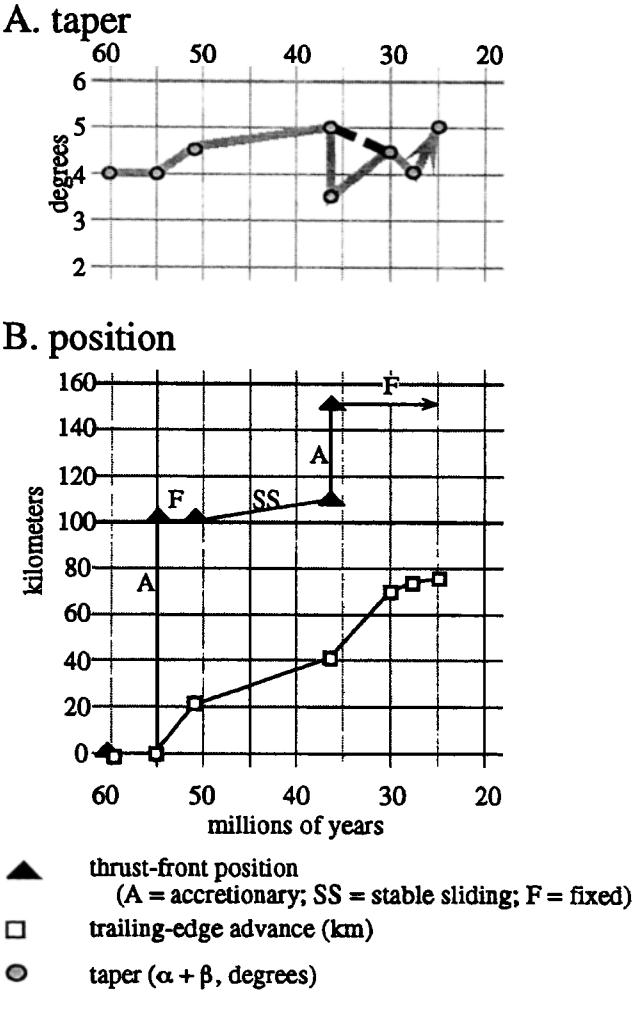

Figure 13. Summary plot of (α) taper angle (a is the topographic slope and b is the dip of the basal detachment) and (β) thrust front and trailing-edge advance (in kilometers (km)). The taper history Between 36 and 30 Ma depends on whether the accreted material is considered part of the wedge instantaneously (shaded, solid line) or progressively (bold, dashed line). See text for discussion. Note that after 30.0 Ma taper decreases until 28 Ma because of internal deformation. Taper rebuilds after 28 Ma because of aggradation of material on to the top of the thrust wedge. Trailing-edge advance occurs continuously, although at variable rates, throughout the deformation. Between 51 Ma and 36 Ma, the slope of the trailing curve is greater than the thrust-front advance curve reflecting concurrent internal deformation.

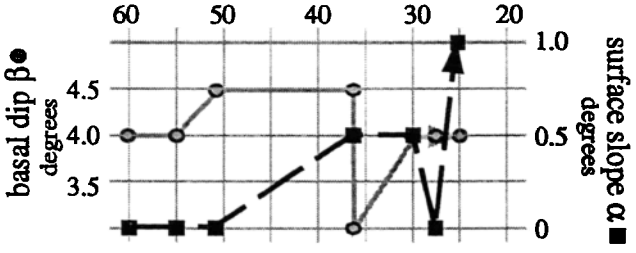

Figure 14. Plot of the surface slope (α, bold dashed line and solid boxes) versus dip of the basal décollement (β, shaded solid line and shaded circles) during each developmental stage of the thrust belt. See Figure 13A for a plot of α + β with time. Note that surface slope (α) varies between 0° and 1° and basal décollement angle (β) varies between 3.5° and 4.5°. Because variations in surface slope and basal dip are not coordinated, it is concluded that they are decoupled and vary independently.

positive, foreland-sloping topographic surface was first established after 51 Ma (Figure 14). Significant structural relief created in the rear of the wedge because of the formation of the Montsec thrust and displacement of the rear of the wedge up the basal décollement created a 0.5° surface slope (Figure 10). Although the dip of the basal décollement remained constant from 51 until 36 Ma, initial translation of the thrust belt on its basal detachment by displacement of the Sierras Marginales thrust southward from its footwall cutoff likely drove continued basement subsidence. At any position in the underthrust basement, the overlying wedge thickened by ~1 km (due to translation) and resulted in ~800 m of basement subsidence (Figures 11b and 10b).

A steady increase in taper angle from 4.5° at 51 Ma to 5° at 36 Ma (+/- 0.5°) is inferred (Figure 13). The relationship between thrust-front advance, internal deformation, and taper until 36 Ma can be summarized as follows (Figures 13 and 14): (1) A thrust-front advance by accretion at 55 Ma was followed by internal deformation and taper building until 51 Ma. (2) Stable-sliding thrust-front advance until 36 Ma was accompanied by additional internal deformation and development of a foreland-sloping upper surface that increased the taper to 5° by 36 Ma. Note that the 55-51 Ma sequence of events is qualitatively compatible with a critical-taper wedge-like evolution (compare Figures 2 and 13), but explanation of the taper increase accompanying stable sliding during the 51-36 Ma interval requires either a decrease in pore fluid pressure or strength contrast between material of the wedge and of the basal décollement.

The final thrust-front advance occurred by accretion at ~36 Ma when the detachment at the base of the foreland-basin sequence was activated ~40 km south of its pre-36-Ma position (Figure 13) [*Meigs et al.*, 1996]. Because the most forelandward structure began forming at this time, all subsequent shortening occurred on the hinterland side of the thrust front. Accretion of the foreland poses a dilemma for defining the 36-Ma, postaccretion wedge taper. Whereas a constant-slope upper surface is defined as the line that connects the high point at the rear of the wedge with the thrust front, the basal décollement has strong curvature separating a 4.5° from a 1° reach beneath the thrust belt to the north and the undeformed foreland to the south, respectively (Figure 10). Projection of a line connecting the base of the rear of the wedge with the thrust front defines an average dip, 3°, which overestimates the dip of the décollement beneath the foreland and underestimates the dip beneath the northern thrust belt. If this projection method is chosen, the taper instantaneously drops to 3.5° at 36 Ma (Figure 13). Alternatively, if the dip of décollement beneath the deformed thrust belt is used, the taper remains unchanged at 36 Ma. Explicit distinction is not purely semantic as it determines how internal deformation affects subsequent changes in wedge geometry. Although the latter interpretation implies that the taper angle smoothly decreased with time, we define the wedge as the average envelope whose toe is the thrust front. Wedge taper drops from 5° to 3.5° after accretion at 36 Ma and subsequently rebuilds (Figure 13).

Significant basement subsidence and a decrease in mean décollement angle accompanied deformation after 36 Ma (Figures 10b, 9b, and 14). The single greatest shortening event during thrust-belt construction, the 29-km translation of the Sierras Marginales thrust sheet over the foreland, occurred during this interval (Figures 7 and 9). Emplacement of the thrust sheet occurred on the hinterland side of the thrust front. Near the thrust front, a minor amount of shortening was absorbed by folding in the accreted foreland. Several important implications arise from comparison of the 36 and 30 Ma reconstructions (Figures 9 and 10, respectively).

Surface slope remains unchanged between 36 and 30 Ma (0.5°, Figure 14), which implies that structural thickening near the front of the wedge related to emplacement of the Sierras Marginales thrust sheet was balanced by raising of the surface of the rear of the wedge due to translation along the décollement. This allowed the differential relief and the slope between front and rear of the wedge to be sustained between 36 and 30 Ma. The existence of internal deformation on the hinterland side of the thrust front, because it is a means building surface slope and recovering critical taper, is often cited as circumstantial evidence for the applicability of critical-taper wedge models (assuming the basal décollement angle remained unchanged) [*Davis et al.*, 1983; *Boyer and Geiser*, 1987; *Geiser and Boyer*, 1987; *Woodward*, 1987; *Morley*, 1988; *Lucas*, 1989; *Dahlen*, 1990; *Boyer*, 1992; *Burbank et al.*, 1992b; *DeCelles et al.*, 1993; *DeCelles*, 1994; *DeCelles and Mitra*, 1995]. In this case, taper angle was recovered largely because of a change in the average basal décollement angle from 4.5° before 36 Ma to 4° at 30 Ma; internal deformation served to sustain the 0.5° surface slope. Finally, although a clear tectonic subsidence of the basement can be seen (Figure 9b), the decreased basal décollement angle suggests that displacement of the wedge onto crust with greater flexural rigidity. This inference is supported by the fact that thinning of the lower crust northward of the Montsec thrust was observed on the ECORS profile [*Muñoz*, 1992].

Hanging wall deformation localized at the southern edge of the Sierras Marginales thrust sheet corresponds with a decrease in taper angle between 30 and 28 Ma (Figures 8, 9, and 13). A moderate amount of shortening was accommodated by reactivation of preexisting thrusts and folds (Figure 8). Like the 36-30 Ma window, shortening was concentrated near the leading edge of the thrust belt. Structural relief created at this time by further growth of the Canelles anticline and thrust faulting at the toe of the Sierras Marginales thrust sheet, despite the fact that the thrust sheets were relatively thin (in some cases less than 300 m thick, compare Figures 8 and 9), was sufficient to decrease the

differential relief between the front and rear of the wedge and resulted in a decrease of the surface slope to 0°. We infer that the basal décollement remained constant after 30 Ma (Figures 6, 8, 9, and 14) recognizing that the amount of structural thickening along the profile for each step varied slightly in detail, causing minor differential tectonic subsidence and modification of the décollement angle. Sediments deposited between 30 and 28 Ma (unit 1, Figure 5) are characterized by lacustrine facies and rapid sediment-accumulation rates [*Meigs et al.*, 1996; *Meigs*, 1997]. In addition to structural damming by the uplift of basin-margin structures [*Ori and Friend*, 1984; *Burbank and Beck*, 1991a, b; *DeCelles et al.*; 1991; *Coogan*, 1992; *Talling et al.*, 1995; *Burbank et al.*, 1996], an overall regional lowering of the average surface slope may have played an important role in the development of rapidly accumulating lakes in the piggy back basins.

A foreland-sloping topographic surface (1°) was reestablished after 28 Ma, whereas the basal décollement angle remained unchanged (4°, Figure 14). Minor internal deformation after 28 Ma is reflected by further folding in the foreland and displacement on the Montargull thrust (Figure 6). Regionally distributed aggradation and backfilling by the youngest alluvial, fluvial, and lacustrine unit (unit 3; Figure 4) is observed on top of the thrust belt after 28 Ma (Figure 6) [*Mellere*, 1992, 1993; *Vergés*, 1993; *Meigs et al.*, 1996; *Meigs*, 1997]. This period of aggradation reflects trapping of sediment derived from the foreland fold-and-thrust belt and from the axial zone. The negligible surface slope at 28 Ma may have facilitated, in part, widespread deposition on top of, rather than bypassing of, the thrust belt. Erosion in the axial zone and development of graded depositional systems across the fold-and-thrust belt were therefore responsible for construction of the 1° surface slope after 28 Ma. Uplift of strata, erosion, and deposition in actively deforming thrust belts are complex processes whose effects vary according to the organization of drainage systems, the erodability of uplifting strata, and the availability of accommodation space [*Burbank and Beck*, 1991a, b; *DeCelles et al.*, 1991, 1993; *Coogan*, 1992; *Burbank and Vergés* 1994; *DeCelles*, 1994; *Lawton et al.*, 1994; *DeCelles and Mitra*, 1995; *Talling et al.*, 1995; *Burbank et al.*, 1996].

We can make a first-order approximation of the topography for each of our time steps but are unable to characterize the structural relief exactly, at specific points in time, on any individual structure. Preservation of anticlinal crests indicates that the rate of uplift was greater than the rate of erosion for each individual structure, but a unique crestal uplift rate for each fold can not be defined. Estimating the error introduced by assuming a mean slope, particularly if local topography varied substantially with time, is problematic. Topographic slopes estimated for each step are a minimum and potentially slightly underestimate the true taper given uncertainty in incremental structural relief. It seems likely that the durability, or relative resistance to erosion [*DeCelles and Mitra*, 1995], of the upper surface changed only in the regions of the Canelles anticline and Montargull thrust where Triassic evaporites are exposed (Figure 6). Over the rest of the thrust belt, Mesozoic carbonates are exposed in the cores of anticlines (Figures 4 and 6). It can be inferred therefore that the rate of erosion across the width of the foreland fold-and-thrust belt did not vary significantly as a consequence of progressive unroofing.

Sequential restoration and reconstruction of taper angle is ambitious. Uncertainties, and potential sources of error, consequently, in taper reconstruction arise from (1) a discontinuous structural and stratigraphic record, (2) variable resolution of age data, (3) uncertainty in absolute values of basal décollement dip and surface slope with time, (4) criteria for determining surface slope, (5) changes in structural relief due to the interplay between erosional lowering and structural uplift of anticlinal crests, (6) isostatic adjustments due to tectonic and sedimentary loading and erosional unloading, and (7) variations in flexural rigidity of the underthrusting plate. Because both stratigraphic thicknesses and the structural evolution of major structures are well constrained [*Pocovi*, 1978a, b; *Meigs et al.*, 1996; *Meigs*, 1997], we are confident that the reconstructed taper angles are representative of relative changes in taper with time.

In contrast, we have variable confidence in the reliability of the absolute values for basal décollement and surface slope angles. For example, in time windows where paleohorizontal stratigraphic data such as the Lower Eocene marine strata or Paleocene strata used to reconstruct the 51-Ma and pre-55-Ma surfaces, respectively, the restorations represent reliably the likely surface and basal slopes (Figures 11 and 12). In contrast, where the surface slope was generalized as a line connecting the rear of the wedge with the thrust front in the spirit of *Davis et al.* [1983], this envelope describes the mean differential relief but is not an envelope of maximum, minimum, or mean elevation. Differential structural-relief approximations of the surface slope, such as the one we used, demonstrate the coupling between structural evolution and surface slope and are an adequate approximation for our purposes. Attempts to investigate the role of topography in the structural development of thrust belts need to reconstruct "true" topographic attributes, that is, mean depositional slope, however [*Beaumont et al.*, 1996].

How does the coupling between advance of the thrust front and internal deformation within the Pyrenean orogenic wedge compare to the coupling predicted for an "ideal" critical-taper wedge? In contrast to an ideal stable-sliding advance (time interval t_1-t_2, Figure 2b), internal deformation accompanied the one stable-sliding advance between 51 and 36 Ma, causing the surface slope to increase by 0.5° (Figure 13). Thrust-front advances by accretion at 55 and 36 Ma were each followed by internal deformation (time interval t_0-t_1, Figure 2), although the style of internal deformation and resultant taper angle associated with each deformational pulse was different (Figures 13 and 14). After 55 Ma, folding across the width of the thrust belt created a wedge with a 0° surface slope and 4.5° basal décollement. After 36 Ma, wedge taper shows considerable instability until the end of deformation after 28 Ma (Figure 14). Translation of a single thrust sheet (~29 km) between 36 and 30 Ma created a 4.5°-tapered wedge. Interestingly, taper recovered not from an increase in surface slope driven by internal deformation (surface slope was 0.5° at 36 and 30 Ma, Figures 10 and 9) but because of a decrease in the basal décollement angle from 4.5° to 4° (Figure 14). Translation of an existing tectonic load to the south onto stronger crust may account for the decreased angle. Surface slope drops to 0° and taper is reduced to 4° at 28 Ma as a consequence of continued thickening near the toe of the wedge. Erosion of the hinterland probably lowered the surface slope of the hinterland after 28 Ma but delivered material to the thrust belt. Aggradation

of hinterland-derived detritus within the thrust belt was sufficient to create a 1° forelandward sloping upper surface (Figure 6).

Inability to constrain pore fluid pressures and variations in mechanical properties limits the ability to compare the Pyrenees, or any orogen, with the critical taper-wedge model. Elevated pore fluid pressure lowers the slope of the critical taper envelope. It seems certain that pore fluids played a role in the development of this thrust belt as it evolved from a submarine to a subaerial belt with time. More explicit definition of the role is difficult in as much as very few pore fluid pressure data are available for active subaerial thrust belts [*Davis et al.*, 1983], and it is difficult to estimate fluid pressure conditions in ancient thrust belts [*DeCelles and Mitra*, 1995]. Qualitatively, a rapid thrust-front advance may elevate pore fluid pressures and create a self-generating feedback loop whereby fault propagation is facilitated by and causes continued generation of pore fluid pressure (D. Davis, personal communication, 1996). Because generation of pore fluid pressure in such a scenario is both nonlinear and nonsteady state, exact, quantitative comparison between taper evolution and structural development of thrust belts is problematic at best and should be treated with skepticism. In contrast, reasonable qualitative inferences of the strength of the wedge and the basal layer are possible [*DeCelles and Mitra*, 1995].

It seems likely that the strength of both the wedge and the basal layer showed little variability with time because of the relatively shallow depth of emplacement, lack of fabric development, and the homogenous character of the material within the wedge (dominated by massive carbonates). A relatively high strength contrast can be inferred between the carbonates within the wedge and the evaporites within which the basal décollement localized. It has been argued that the critical-taper envelope for thrust belts above evaporite detachments, like the Pyrenees, have extremely low slopes ($\alpha + \beta = 1°$-$2°$ [*Davis et al.*, 1983; *Davis and Engelder*, 1985; *Jaumé and Lillie*, 1988; *Davis and Lillie*, 1994]). Clearly the observed magnitude of the internal deformation would not have been predicted from either the initial stratigraphic taper or the deformed-state taper of 4° and 4°-5°, respectively [*Davis and Engelder*, 1985; *Jaumé and Lillie*, 1988; *Lawton et al.*, 1994; *Davis and Lillie*, 1994]. Furthermore, comparable amounts of internal deformation are seen in this study and on the ECORS profile [*Muñoz*, 1992; *Vergés*, 1993]. This, too, is an unexpected result because stratigraphic wedges with greater initial taper, such as along the ECORS transect (5°, [*Muñoz*, 1992]), should have systematically less internal deformation because initially they are close to critical taper [*Lawton et al.*, 1994].

The internal and external evolution of the Pyrenees between 55 and 28 Ma were coupled, but the topographic slope and the basal décollement angles were decoupled (Figure 14). Rather than revolving around maintenance of a fundamental taper angle, taper angle was primarily controlled by relative rates of creation of structural relief, the flexural rigidity of the lower plate, and the taper of the pretectonic stratigraphic wedge. The relative rate of change in structural relief at the toe versus the rear of the thrust belt determined the average surface slope, except after 28 Ma when aggradation caused a 1° increase in surface slope. When the rate of relief created by translation of the rear of the wedge up the décollement exceeded the rate of relief created by deformation at the toe of the wedge, such as between 51 and 36 Ma (Figure 14), the surface slope increased. When the rate was greater at the toe, slope angle decreased, for example, between 30 and 28 Ma. When the rate that structural relief is created at the toe balanced that at the rear, the surface slope remained unchanged. Overthrusting of the foreland between 36 and 30 Ma, internal deformation that accounts for nearly 40% of the total shortening and coinciding with translation of the thrust belt onto a lower-angle portion of the basal décollement, caused a decrease in wedge taper because the topographic slope remained constant (Figures 9 and 10).

Consideration of the 51-Ma reconstruction demonstrates the role of stratigraphy in the spatial partitioning of deformation during initial deformation (Figure 11). A thrust-belt-wide fold train, a series of folds whose wavelength and amplitude decrease systematically toward the foreland, characterize the first-formed structure. A systematic decrease in fold wavelength and amplitude corresponds with an overall southward thinning of the pretectonic stratigraphic succession (Figure 5). Subsequent deformation was localized at these sites of initial folding. Experimental folding of materials with various strength contrasts confirm the importance of the initial stratigraphic succession in the internal geometry, partitioning of deformation, and creation of structural relief [*Currie et al.*, 1962; *Dixon and Tirrul*, 1991; *Liu and Dixon*, 1991; *Dixon and Liu*, 1992]. Clearly, the pretectonic stratigraphic sequence acted as a first-order control on the sites of subsequent deformation.

Observations and their interpretation are aided by models, such as the critical-taper wedge model, because they provide a theoretical framework within which interrelationships may be explored [*Beaumont et al.*, 1996]. Our goal has not been to determine whether wedge models are right or wrong but rather to explore the interplay between internal structural evolution, surface slope evolution, and basal décollement angle as the Pyrenean foreland fold-and-thrust belt was emplaced. In some ways, the Pyrenees appear to behave like a critically tapered wedge. For example, accretion lowers taper and is followed by a period of taper reconstruction. In other ways, the coupling between internal deformation, surface slope development, and basal décollement angle are not simply related. Internal deformation caused basement subsidence without building surface slope. Taper angle was maintained and even lowered because internal deformation was insufficient to build slope with contemporaneous translation on to stronger crust. Given that the mechanical characteristics of foreland fold-and-thrust belts diverge from those assumed in the critical-taper wedge model [*Bombolakis*, 1994], additional high-resolution studies of the spatial, temporal, and geometrical evolution of thrust belts are needed to understand the coupling between their internal and external development. Modeling strategies that consider larger, plate boundary scale interactions of denudation, mantle subduction, subduction load, coupling between crust and mantle, crustal delamination, and shear zone strength are likely to provide greater insight into orogenic processes than studies that focus on one element (the thrust belt) of a larger, coupled system [*Royden and Burchfiel*, 1989; *Willett*, 1992; *Vergés*, 1993; *Willett et al.*, 1993; *Beaumont et al.*, 1996].

Acknowledgments. Supported by NSF grant EAR-9304863 and grants from the Donors of the Petroleum Research Fund (ACS-28270-AC) to D.W.B. A. J. M. was supported by grants from A.A.P.G., G.S.A., and

Sigma Xi and a Shell Foundation Fellowship. The stereonet program was provided by R. Allmendinger. Jaume Vergés, Josep Anton Muñoz, and Ken Fowler are thanked for skepticism and encouragement, discussions, and field and interpretation assistance. Dan Davis and Françoise Roure are thanked for their positive and constructive reviews on behalf of tectonics.

References

Anadón, P., L. Cabrera, F. Colombo, M. Marzo, and O. Riba, -Syntectonic intraformational unconformities in alluvial fan deposits, eastern Ebro Basin margins (NE Spain), in *Foreland Basins*, edited by P. A. Allen and P. Homewood, pp. 259-271, Blackwell Scientific, Oxford, 1986.

Beaumont, C., P. J. J. Kamp, J. Hamilton, and P. Fullsack, The continental collision zone, South Island, New Zealand: Comparison of geodynamical models and observations, *J. Geophys. Res., 101*, 3333-3359, 1996.

Bombolakis, E. G., Applicability of critical-wedge theories to foreland belts, *Geology*, 22, 535-538, 1994.

Boyer, S. E., Geometric evidence for synchronous thrusting in the southern Alberta and northwest Montana thrust belts, in *Thrust Tectonics*, edited by K. R. McClay, pp. 377-390, Chapman and Hall, New York, 1992.

Boyer, S. E., and P. A. Geiser, Sequential development of thrust belts: implications for mechanics and cross section balancing, *Geol. Soc. Am. Abstr. Progs., 19*, pp. 597, 1987.

Burbank, D. W., and R. A. Beck, Early Pliocene uplift of the Salt Range: Temporal constraints on thrust wedge development, northwest Himalaya, Pakistan, *Spec. Pap. Geol. Soc. Am., 232*, 113-128, 1989.

Burbank, D. W., and R. A. Beck, Models of aggradation versus progradation in the Himalayan Foreland, *Geol. Rundsch., 80*, 623-638, 1991.

Burbank, D. W., and R. A. Beck, Rapid, long-term rates of denudation, *Geology, 19*, 1169-1172, 1991.

Burbank, D. W., and J. Vergés, Reconstruction of topography and related depositional systems during active thrusting, *J. Geophys. Res., 99*, 20,281-20,297, 1994.

Burbank, D. W., C. Puigdefàbregas, and J. A. Muñoz, The chronology of Eocene tectonics and stratigraphic development of the eastern Pyrenean foreland basin, northeast Spain, *Geol. Soc. Am. Bull., 104*, 1101-1120, 1992a.

Burbank, D. W., J. Vergés, J. A. Muñoz, and P. Bentham, Coeval hindward- and forewardimbricating thrusting in the south-central Pyrenees, Spain: Timing and rates of shortening and deposition, *Geol. Soc. Am. Bull., 104*, 3-17, 1992b.

Burbank, D.W., A. J. Meigs, and N. Brozovic, Interactions of growing folds and coeval depositional systems, *Basin Res., 8*, 199-223, 1996.

Byrne, D. E., W.-H. Wang, and D. M. Davis, Mechanical role of backstops in the growth of forearcs, *Tectonics, 12*, 123-144, 1993.

Byrne, T., and J. Hibbard, Landward vergence in accretionary prisms: The role of the backstop and thermal history, *Geology, 15*, 1163-1167, 1987.

Cande, S. C., and D. V. Kent, A new geomagnetic polarity time scale for the Late Cretaceous and Cenozoic, *J. Geophys. Res., 97*, 13917-13951, 1992.

Chapple, W. M., Mechanics of thin-skinned fold-and-thrust belts, *Geol. Soc. Am. Bull., 89*, 1189-1198, 1978.

Choukroune, P., and M. Seguret, Tectonics of the Pyrenees: Role of compression and gravity, in *Gravity and Tectonics*, edited by K. De Jong and R. Scholten, pp. 141-156, John Wiley, New York, 1973.

Choukroune, P., and ECORS Team, The ECORS Pyrenean deep seismic profile reflection data and the overall structure of an orogenic belt, *Tectonics, 8*, 23-29, 1989.

Colletta, B., J. Letouzey,, R. Pinedo, J. F. Ballard, and P. Bale, Computerized X-ray tomography analysis of sandbox models: Examples of thin-skinned thrust systems, *Geology, 19*, 1063-1067, 1991.

Coogan, J. C., Structural evolution of piggyback basins in the Wyoming-Idaho-Utah thrust belt, *Mem. Geol. Soc. Am., 179*, 55-81, 1992.

Currie, J. B., H. W. Patnode, and R. P. Trump, Development of folds in sedimentary strata, *Geol. Soc. Am. Bull., 73*, 655-674, 1962.

Dahlen, F. A., Critical taper model of fold-and-thrust belts and accretionary wedges, *Annu. Rev. Earth Planet. Sci., 18*, 55-99, 1990.

Dahlen, F. A., and J. Suppe, Mechanics, growth, and erosion of mountain belts, *Spec. Pap. Geol. Soc. Am., 218*, 161-178, 1988.

Davis, D. M., and T. Engelder, The role of salt in fold-and-thrust belts, *Tectonophysics, 119*, 67-89, 1985.

Davis, D. M., and R. J. Lillie, Changing mechanical response during continental collision: Active examples from the foreland thrust belts of Pakistan, *J. Struct. Geol., 16*, 21-34, 1994.

Davis, D. M., J. Suppe, and F. A. Dahlen, Mechanics of fold-and-thrust belts and accretionary wedges, J. Geophys. Res., 88, 1153-1172, 1983.

DeCelles, P. G., Late Cretaceous-Paleocene synorogenic sedimentation and kinematic history of the Sevier thrust belt, northeast Utah and southwest Wyoming, *Geol. Soc. Am. Bull., 106*, 32-56, 1994.

DeCelles, P. G., and G. Mitra, History of the Sevier orogenic wedge in terms of critical taper models, northeast Utah and southwest Wyoming, *Geol. Soc. Am. Bull., 4*, 454-462, 1995.

DeCelles, P. G., M. B. Gray, K. D. Ridgway, R. B. Cole, P. Srivastava, N. Pequera, and D. Pivnik, D. A., Kinematic history of a foreland uplift from Paleocene synorogenic conglomerate, Beartooth Range, Wyoming and Montana. *Geol. Soc. Am. Bull., 103*, 1458-1475, 1991.

DeCelles, P. G., H. T. Pile, and J. C. Coogan, Kinematic history of the Meade thrust based on provenance of the Bechler conglomerate at Red Mountain, Idaho, Sevier thrust belt, *Tectonics, 12*, 1436-1450, 1993.

Dixon, J. M., and S. Liu, Centrifuge modelling of the propagation of thrust faults, in *Thrust Tectonics*, edited by K. R. McClay, pp. 53-70, Chapman and Hall, New York, 1992.

Dixon, J. M., and R. Tirrul, Centrifuge modelling of fold-thrust structures in a tripartite stratigraphic succession, *J. Struct. Geol., 13*, 3-20, 1991.

Farrell, S. G., G. D. Williams, and C. D. Atkinson, Constraints on the age of movement of the Montsech and Cotiella Thrusts, south central Pyrenees, Spain, *J. Geol. Soc. London, 144*, 907-914, 1987.

Geiser, P. A., The role of kinematics in the construction and analysis of geological cross sections in deformed terranes, *Spec. Pap. Geol. Soc. Am., 222*, 47-76, 1988.

Geiser, P. A., and S. E. Boyer, The paradox of the orogenic wedge and a model for crustal recycling, *Geol. Soc. Am. Abstr. Programs, 19*, 674, 1987.

Hogan, P. J., Geochronologic, tectonic, and stratigraphic evolution of the southwest Pyrenean foreland basin, northern Spain, Ph.D. thesis, 219 pp., Univ. of Southern California, Los Angeles, 1993.

Jaumé, S. C., and R. J. Lillie, Mechanics of the Salt Range-Potwar Plateau, Pakistan: A fold-and-thrust belt underlain by evaporites, *Tectonics, 7*, 57-71, 1988.

Lawton, T. F., S. E. Boyer, and J. G. Schmitt, Influence of inherited taper on structural variability and conglomerate distribution, Cordilleran fold and thrust belt, western United States, *Geology, 22*, 339-342, 1994.

Liu, S., and J. M. Dixon, Centrifuge modelling of thrust faulting: Structural variation along strike in fold-thrust belts, *Tectonophysics, 188*, 39-62, 1991.

Losantos, M. E., Aragonès, X. Berástegui, and C. Puigdefàbregas, Mapa Geològic de Catalunya, 1:250,00 scale, Institut Cartogràfic de Catalunya, Barcelona, Spain, 1989.

Lucas, S. B., Structural evolution of the Cape Smith thrust belt and the role of out-of-sequence faulting in the thickening of mountain belts, *Tectonics, 8*, 655-676, 1989.

Martínez, A., J. Vergés, and J. A. Muñoz, Sequencias de propagación del sistema de

cabalgamientos de la terminación del manto del Pedraforca y relación con los conglomerados sinorogénicos, *Acta Geol. Hisp., 23*, 119-128, 1988.

Martínez Peña, M. B. and Pocoví, A., El amortiguamiento frontal de la estructura de la cobertera surpirenaica y su relacion con el anticlinal Barbastro-Balaguer, Acta Geol. Hisp., 23, 81-94, 1988.

Meigs, A. J., Sequential development of selected Pyrenean thrust faults, *J. Struct. Geol.*, in press 1997.

Meigs, A. J. and Burbank, D. W., Thrust sheets as a proxy for whole orogens: Testing the critical taper wedge model with an example from the Spanish Pyrenees, *Geol. Soc. Am. Abstr. Programs, 25*, A-230, 1993.

Meigs, A. J., J. Vergés, and D. W. Burbank, Ten-million-year history of a thrust sheet, *Geol. Soc. Am. Bull., 12*, 1608-1625, 1996.

Mellere, D., I Conglomerati di Pobla de Segur: Stratigrafia Fisica e Relazioni Tettonica-Sedimentazione, Ph.D. thesis., 203 pp., Univ. of Padova, Padova, Italy, 1992.

Mellere, D., Thrust-generated, back-fill stacking of alluvial fan sequences, south-central Pyrenees, Spain (La Pobla de Segur Conglomerates), in *Tectonic Controls and Signatures in Sedimentary Successions*, edited by L. E. Frostick and R. J. Steel, pp. 259-276, Blackwell Sci., Cambridge, Mass., 1993.

Misch, P., Der Bau der Mittleren Sudpyrenäen, *Abh. Geselsch. Göttingen Math. Phys. Kl.13*, 1597-1764, 1934.

Morley, C. K., Out-of-sequence thrusts, *Tectonics, 7*, 539-561, 1988.

Mulugeta, G., Modelling the geometry of Coulomb thrust wedges, *J. Struct. Geol., 10*, 847-859, 1988.

Mulugeta, G. and H. Koyi, Three-dimensional geometry and kinematics of experimental piggyback thrusting, *Geology, 15*, 1052-1056, 1987.

Muñoz, J. A., Evolution of a continental collision belt: ECORS-Pyrenees crustal balanced section, in *Thrust Tectonics*, edited by K.R. McClay, pp. 235-246, Chapman and Hall, New York, 1992.

Mutti, E., J. Rosell, G. P., Allen, F. Fonnesu, and M. Sgavetti, The Eocene Baronia tide dominated delta-shelf system in the Ager Basin, in *IAS 6th Regional Meeting Excursion Guidebook*, edited by M. D. Mila and J. Rosell, pp. 579-600, Intl. Assoc. Sediment., Lerida, Spain, 1985.

Mutti, E., M. Seguret, and M. Sgavetti, Sedimentation and deformation in the Tertiary sequences of the southern Pyrenees, in *American Association of Petroleum Geologists Mediterranean Basins Conference Field Trip Guide, 1-153*, Nice, France, 1988.

Ori, G. G., and P. F. Friend, Sedimentary basins formed and carried piggyback on active thrust sheets, *Geology, 12*, 475-478, 1984.

Platt, J. P., Dynamics of orogenic wedges and the uplift of high-pressure metamorphic rocks, *Geol. Soc. Am. Bull., 97*, 1037-1053, 1986.

Pocoví, J., Estudio geologico de las Sierras Marginales Catalanas (Prepirineo de Lerida), Ph.D. thesis, 218 pp., Univ. of Barcelona, Barcelona, 1978a.

Pocoví, J., Estudio geologico de las Sierras Marginales Catalanas (Prepirineo de Lerida), *Acta Geol. Hisp., 13*, 73-79, 1978b.

Price, R. A., The mechanical paradox of large overthrusts, *Geol. Soc. Am. Bull., 100*, 1898-1908, 1988.

Puigdefàbregas, C., J. A. Muñoz, and J. Vergés, Thrusting and foreland basin evolution in the Southern Pyrenees, in *Thrust Tectonics*, edited by K. R. McClay, pp. 247-254, Chapman and Hall, New York, 1992.

Riba, O., Syntectonic unconformities of the Alto Cardener, Spanish Pyrenees: A genetic interpretation, *Sediment. Geol., 15*, 213-233, 1976.

Roure, F., P. Choukroune, X. Berastegui, J. A. Muñoz, A. Villien, P. Matheron, M. Bareyt, M. Seguret, P. Camara, and J. Deramond, ECORS deep seismic data and balanced cross sections: Geometric constraints on the evolution of the Pyrenees, *Tectonics, 8*, 41-50, 1989.

Royden, L., and B. C. Burchfiel, Are systematic variations in thrust belt style related to plate boundary processes? (The western Alps versus the Carpathians), *Tectonics, 8*, 51-61, 1989.

Sáez, A., J. Vergés, J. J. Pueyo, J. A. Muñoz, and P. Burquets, Eventos evaporíticos paleógeneos en la cuenca de antepaís surpirenaica: Causas climáticas- causus tectónicas?, in *Libro-Guía Excursion 5 II Congreso del Grupo Español del Terciaro*, edited by F. Colombo, pp. 85, Vic, Spain, 1991.

Senz, J.G. and M. Zamorano, Evolución tectónica y sedimentaria durante el Priaboniense superior-Mioceno inferior, en el frente de cabalgamientos de las Sierras Marginales occidentales, *Acta Geol. Hisp., 27*, 195-209, 1992.

Simó, A, and C. Puigdefàbregas, Transition from shelf to basin on an active slope, upper Cretaceous, Tremp area, southern Pyrenees, in *6th European Regional Meeting Excursion Guide-book*, pp. 63-108, Intl. Assoc. of Sediment., Lleida, Spain, 1985.

Stockmal, G. S., Modeling of large-scale accretionary wedge deformation, J. *Geophys. Res., 88*, 8271-8287, 1983.

Sudre, J., et al., La biochronologie mammalienne du paléogène au Nord et au Sud des Pyrénées: Etat de la question, *C. R. Acad. Sci. Sèr. II, 314*, 631-636, 1992.

Talling, P. J., T. F. Lawton, D. W. Burbank, and R. S. Hobbs, Evolution of latest Cretaceous-Eocene nonmarine deposystems in the Axhandle piggyback basin of central Utah, *Geol. Soc. Am. Bull., 107*, 297-315, 1995.

Teixell, A., Estructura alpina en la transversal de la terminacion occidental de la Zona Axial Pirenaica, Ph.D. thesis, 252 pp., Univ. de Barcelona, Barcelona, 1992.

Vergés, J., Estudi tectònic del vessant sud del Pirineu oriental i central: Evolució cinemàtica en 3D, Ph.D. Thesis, 203 pp., Universitat de Barcelona, Barcelona, 1993.

Vergés, J., and J. A. Muñoz, Thrust sequences in the southern central Pyrenees, *Bull. Soc. Geol. Fr., 8*, 399-405, 1990.

Vergés, J., J. A. Muñoz, and A. Martínez, South Pyrenean fold-and-thrust belt: Role of foreland evaporitic levels in thrust geometry, in *Thrust Tectonics*, edited by K. R. McClay, pp. 255-264, Chapman and Hall, New York, 1992.

Vergés, J., H. Millán, E. Roca, J. A. Muñoz, M. Marzo, J. Cirés, T. den Bezemer, R. Zoetemeijer, and S. Cloetingh, Eastern Pyrenees and related foreland basins: Pre-, syn-, and post-collisional crustal-scale cross-sections, *Mar. Pet. Geol., 12*, 903-915, 1995.

Vergés, J., D. W. Burbank, and A. J. Meigs, Unfolding: An inverse approach to fold kinematics, *Geology, 24*, 175-178, 1996.

Willett, S. D., Dynamic and kinematic growth and change of a Coulomb wedge, in *Thrust Tectonics*, edited by K. R. McClay, pp. 19-32, Chapman and Hall, New York, 1992.

Willett, S., C. Beaumont, and P. Fullsack, Mechanical models for the tectonics of doubly vergent compressional orogens, *Geology, 21*, 371-374, 1993.

Williams, G. D., Thrust tectonics in the south central Pyrenees, *J. Struct. Geol., 7*, 11-17, 1985.

Williams, G. D., and M. W. Fischer, A balanced cross-section across the Pyrenean orogenic belt, *Tectonics, 3*, 773-780, 1984.

Woodward, N. B., Geological applicability of critical-wedge thrust-belt models, *Geol. Soc. Am. Bull., 99*, 827-832, 1987.

D. W. Burbank, Department of Earth Sciences, University of Southern California, Los Angeles, CA 90089-0740. (email: burbank@usc.edu)

A. J. Meigs, Division of Geological and Planetary Sciences, California Institute of Technology, Pasadena, CA 91125. (email: meigs@gps.caltech.edu)

(Received May 29, 1996;
revised November 12, 1996;
accepted November 20, 1996.)